

# UNCLASSIFIED

AD NUMBER
AD842501
NEW LIMITATION CHANGE
TO Approved for public release, distribution unlimited
FROM Distribution authorized to U.S. Gov't. agencies and their contractors; Critical Technology; 15 OCT 1968. Other requests shall be referred to Aero Propulsion Lab., Wright-Patterson AFB, OH 45433.
AUTHORITY
AFAPL ltr, 12 Apr 1972

THIS PAGE IS UNCLASSIFIED

AD 842501

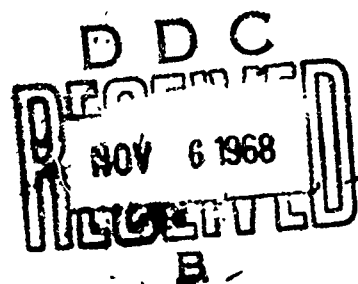
Contract No. AF33(613)-3487

Covering the Period

1 July 1968 to 1 October 1968

SILVER-ZINC ELECTRODES  
AND  
SEPARATOR RESEARCH

Ninth Quarterly  
Technical Progress Report  
Dated  
October 15, 1968



RESEARCH #2 UNCLASSIFIED

This document is subject to special export controls and each transmittal to foreign governments or foreign nationals may be made only with prior approval of AFAPL

*Flight Vehicle Power Br. 2B-P.A.F.B. Plus 45423*

Prepared by

J. A. Kerala

Delco-Remy Division, General Motors Corporation

Including

DR-115475 Preparation and Characterization of Special Zinc Oxides for Evaluation in Silver Oxide-Zinc Secondary Batteries  
D. O. Carpenter and G. E. Snow  
New Jersey Zinc Company

DR-108650 Influence of Membrane Transport Characteristics on Electrolyte Concentration and Consequent Plate Performance, Final Report  
A. H. Remanick, M. Shaw and W. L. Nelson  
Whittaker Corporation

## NOTICE

Foreign announcement and distribution of this report is not authorized. Release to the Clearinghouse for Federal Scientific and Technical Information, EFSTI (formerly OTS) is not authorized. The distribution of this report is limited because it contains technology identifiable with items on the Strategic Embargo Lists excluded from export or re-export under U. S. Export Control Act of 1949 (63STAT.7), as amended (50 USC APP 2020.2031), as implemented by AFR 400-10.

## FOREWORD

This report was prepared by Delco-Remy Division of General Motors Corporation, Anderson, Indiana, on Air Force Contract No. AF33(615)-3487, Silver-Zinc Electrodes and Separator Research. The work was administered under the direction of the Static Energy Conversion Section, Flight Vehicle Power Branch, Aero-Space Power Division, Aero Propulsion Laboratory; Mr. J. E. Cooper was task engineer for the laboratory.

The assistance of Dr. T. P. Dirkse, Professor of Chemistry, Calvin College, Grand Rapids, Michigan, as consultant on this project is greatly appreciated.

This report is being published and distributed prior to Air Force review. The publication of this report, therefore, does not constitute approval by the Air Force of the findings or conclusions contained herein. It is published for the exchange and stimulation of ideas.

## TABLE OF CONTENTS

	<u>Page</u>
I. <u>Introduction</u> . . . . .	1
II. <u>Factual Data</u> . . . . .	2
A. <u>Separators</u> . . . . .	2
B. <u>Particle Size and Morphology of Zinc Oxide</u> . . . . .	5
C. <u>Zinc Electrode Fabrication Techniques</u> . . . . .	6
D. <u>Influence of Membrane Separator Characteristics</u> . . . . .	7
III. <u>Summary</u> . . . . .	7

## ABSTRACT

25 a.h. cells are under cycle test containing 90 Mrad crosslinked methacrylic acid radiated graft. These cells contain three, four and five layers of this membrane. Cells constructed with rectangular voids at the plate centers have been cycled at 60% DOD with some success, but in general the results have not been exceptional.

Cells containing .3% Al doped ZnO and .25% Pb doped ZnO as negative active material delivered 212 and 190 cycles respectively at 60% DOD.

## I. Introduction

The specific items under study in this contract are:

- A. Separators
- B. Electrolytes
- C. Mechanical Barriers to Zinc Agglomeration
- D. Particle Size and Morphology of Zinc Oxide
- E. Zinc Electrode Fabrication Techniques
- F. Influence of Membrane Separator Characteristics
- G. Sites for Zinc Oxide Overgrowth
- H. Development of Failure Analysis Technique
- I. Sizes of Zincate Ion and Soluble Silver Species  
in KOH
- J. Membrane Pore Size Measurements in KOH
- K. Stoichiometric Ratio of Formed Zinc
- L. Fundamental Studies on Surfactants
- M. Alternate Method of Surface Area Measurement
- N. Surfactant Tests

The cycle used in this program is a 35 minute discharge at 20 amperes with an 85 minute recharge to constant voltage.

This report covers the first three-month period of the third year on this program.



## II. Factual Data

### A. Separators

The results of the tests on cells containing four layers of RAI 90 Mrad crosslinked acrylic and methacrylic acid graft performed at the Quality Assurance Laboratory at Crane, Indiana are compared with those obtained at Delco-Remy.

#### 1. Cells containing 4 layers of acrylic acid graft.

<u>DOD</u>	<u>Cell #</u>	<u>Crane</u>	<u>Delco-Remy</u>
25%	1	203*	324*
	2	369*	324*
	3	357*	300 <sup>1</sup>
40%	4	84*	144*
	5	84*	144*
	6	84*	144*
60%	7	34*	84*
	8	34*	84*
	9	34*	84*

#### 2. Cells containing 4 layers methacrylic acid graft.

<u>DOD</u>	<u>Cell #</u>	<u>Crane</u>	<u>Delco-Remy</u>
25%	1	215 <sup>1</sup>	400*
	2	237 <sup>1</sup>	428*
	3	237 <sup>1</sup>	428*
40%	4	84*	253*
	5	84*	253*
	6	84*	253*
60%	7	34*	72*
	8	34*	72*
	9	34	72*

### 3. Control cells containing 4 layers FSC

<u>DOD</u>	<u>Cell #</u>	<u>Crane</u>	<u>Delco-Remy</u>
25%	1	100 <sup>c</sup>	396*
	2	100 <sup>c</sup>	396 <sup>1</sup>
	3		480 <sup>1</sup>
	4		528 <sup>1</sup>
40%	1	100*	228*(2)
	2	100*	312*(2)
60%	1	38*	156*(4)
	2	38*	

\* = failure by loss of capacity  
 1 = failure by short circuiting  
 () = number of cells  
 c = cycling

Cells have been constructed with the 5000 foot lot of 90 Mrad crosslinked methacrylic acid radiation graft utilizing three, four and five layers. Each cell contains nineteen plates, so that no shimming is required. The control cells contain fifteen plates and four layers of FSC.

These cells have been activated in 50% KOH and are under cycle test. The following table shows the initial capacities obtained.

<u>No. of Cells</u>	<u>No. of Layers</u>	<u>Initial Capacity</u>
8	3	35.8 ah
8	4	37.0 ah
8	5	36.0 ah
6 controls	4 FSC	24.0 ah

The cells containing three and four layers are to be cycled at QAL, Crane, Indiana.

Additional cells containing three, four and five layers of RAI membrane will be constructed with zinc oxides containing Pb and Al.

The general physical appearance of this 5000 foot lot of RAI material is excellent. The resistivity checks are within the 60 milliohms in<sup>2</sup> readings obtained by RAI personnel. Additional membrane checks are underway to determine zinc and silver diffusion, and zinc penetration.

The final report by RAI Inc. will be forthcoming shortly, and will be incorporated in the Tenth Quarterly Report.

8. Particle Size and Morphology of Zinc Oxide

25 ah cells containing negative plates with .25% Pb doped zinc oxide and .3% Al doped zinc oxide have completed life cycle tests as follows:

<u>No. of Cells</u>	<u>Doped ZnO</u>	<u>Initial Capacity</u>	<u>Cycles @ 60% DOD</u>
20	.3% Al	23 ah	212
20	.25% Pb	24 ah	180
12 controls	Kadox 15	20 ah	110

The main cause of failure was loss of negative capacity. Additional cells were constructed with Zn flake as negative active material. These cells only delivered 60 cycles at 60% DOD. A continuation of cycling at 25% DOD yielded 440 cycles. The cause of failure here was excessive short circuiting.

An additional 75 lbs. of each doped ZnO is on hand for cell construction incorporating the radiated polyethylene membrane material by RAI.

A Seventh Quarterly Report by New Jersey Zinc Company is enclosed.

C. Zinc Electrode Fabrication Techniques

An experimental 25 a.h. cell containing three layers of FSC membranes was constructed as follows:

All the negative plates had a center section removed in the shape of a rectangle, and a plastic shim was inserted in the cavity. This area was 2" x 3/4". Additional plates were utilized in the element such that the surface area of active material was the same as in regular 25 a.h. cell construction. This cell delivered 290 cycles at 60% DOD.

However, additional cells constructed with standard 25 a.h. size plates having a smaller opening at the plate centers only yielded 130 cycles at 60% DOD.

Additional cells are under construction to try and optimize the hole size which seems to prohibit the zinc material from agglomerating at the plate centers to limit life.

The main cause of a failure in these cells was excessive washing of the zinc material.

D. Influence of Membrane Separator Characteristics

A final report by the Whittaker Corporation is attached.

III. Summary

The 5000 foot production run by RAI Inc. of a 90 Mrad crosslinked methacrylic acid radiation grafted membrane is under test both in cells and in certain screening conditions. The use of this separator has made possible the addition of four extra plates per cell in the standard 25 ah container. These cells are to be cycled at 60% DOD.

Cells containing ZnO doped with .3% Al and .25% Pb have delivered 212 and 190 cycles respectively at 60% DOD. Additional cells are under construction with this material utilizing RAI membranes.

Cells containing rectangular voids at the plate centers have shown some promise to extend cycle life at 60% DOD. Additional work is underway to definitely determine the correct void size that will be most beneficial to plate cycle life.

Purchase Order D-R115475  
Under Contract No. AF33(615)-3487

PREPARATION AND CHARACTERIZATION OF SPECIAL  
ZINC OXIDES FOR EVALUATION IN  
SILVER OXIDE-ZINC SECONDARY BATTERIES

Seventh Quarterly Technical Progress Report

Covering the Period

15 April 1968 to 15 July 1968

Dated

17 July 1968

Prepared by

D. O. Carpenter

G. E. Snow

## FOREWORD

This report was prepared by The New Jersey Zinc Company, Palmerton, Pennsylvania on Delco-Remy Division of General Motors Corporation Purchase Order D-R115475 under Air Force Contract No. AF33(615)-3487. The work was directed by Drs. C. E. Barnett and L. J. Reimert.



# NOTICE

Foreign announcement and distribution of this report is not authorized. Release to the Clearinghouse for Federal Scientific and Technical Information, CFSTI (formerly OTS) is not authorized. The distribution of this report is limited because it contains technology identifiable with items on the Strategic Embargo Lists excluded from export or re-export under U.S. Export Control Act of 1949 (63STAT.7), as amended (50 USC APP 2020.2J31), as implemented by AFR 400-10.

This report is being published and distributed prior to Air Force review. The publication of this report, therefore, does not constitute approval by the Air Force of the findings or conclusions contained herein. It is published for the exchange and stimulation of ideas.

## TABLE OF CONTENTS

I. Introduction .....	Page 1
II. Sample Characterization Tests .....	1
III. Description of Sample Preparation .....	2
IV. Future Program .....	2
V. Appendix .....	2

LIST OF TABLES

Table 1 Characterization Data for Pb- and Al-doped ZnO and  
Flaked Zn-dust Samples

Page 3

LIST OF FIGURES

V. Appendix

<u>Figure</u>	<u>Sample No.</u>	<u>Description</u>
1	243-107-5	Electron Micrograph of Pb-doped ZnO
2	243-41-2	Electron Micrograph of Al-doped ZnO
3	243-123-2	Optical Micrograph of Flaked Zn-dust

# ABSTRACT

Previous evaluations of Zn electrodes fabricated with Pb-doped ZnO or flaked Zn-dust indicated that these materials would increase the cycle-life of silver oxide-zinc secondary batteries. Interesting results were also obtained with High Conductivity Al-doped ZnO. Thus, twenty-five pounds of each of these samples have been prepared for more comprehensive performance evaluations by Delco-Remy.

## I. Introduction

The objective of this project has been to prepare and characterize a variety of zinc oxides and zinc dusts for evaluation in silver oxide-zinc secondary batteries. Of the small samples which have been tested, 0.25% Pb-doped ZnO and flaked Zn-dust showed the most promise for increasing the Zn-electrode cycle-life. Samples with 0.03% to 2.5% Pb indicated no advantage for Pb-contents greater than about 0.25%. Flaked Zn-dust was found to be superior to normal Zn-dust.

Al-doping under appropriate conditions leads to a major modification of ZnO in that it increases the electrical conductivity by several orders of magnitude. Although earlier results with Al-doped High Conductivity ZnO have not shown large increases in electrode cycle-life, this type of ZnO is of interest.

During the past quarter, twenty-five pounds of each of the preceding samples have been prepared. This will permit more comprehensive performance evaluations by Delco-Remy.

## II. Sample Characterization Tests

The ZnO samples were characterized by the following tests: (1) air permeability particle size, (2) nitrogen adsorption surface area, (3) electron micrographs, (4) qualitative spectrographic and, where necessary, chemical analysis for specific impurities. See the First Quarterly Report (31 January 1967) for a description of these tests.

The flaked Zn-dust sample was characterized by tests for purity, degree of oxidation to ZnO, and average flake thickness. (See the Fourth Quarterly Report, 23 October 1967 for test method.) Due to the relatively large size of the particles, optical micrographs (100X) were used instead

of electron micrographs to show the particle shape.

### III. Description of Sample Preparations

#### A. Pb-doped ZnO (Sample No. 243-107-5)

This sample was prepared by 600°C. calcination in air of an intimate admixture of French Process ZnO and PbO. It actually is just a larger scale repeat preparation of sample 243-107-1 described in the Third Quarterly Report (17 July 1967). Characterization data are given in Table 1 and Figure 1.

#### B. High Conductivity Al-doped ZnO (Sample No. 243-41-2)

The procedure for doping ZnO with Al so as to develop high electrical conductivity is described in U.S. Patent 3,089,856 by H. M. Cyr and N. S. Nanovic, assigned to New Jersey Zinc Company, and issued 14 May 1963. Characterization data are given in Table 1 and Figure 2.

#### C. Flaked Zn-dust (Sample No. 243-123-2)

The flaked Zn-dust was prepared by the procedure described for sample 243-123-1. (See the Fourth Quarterly Report, 23 October 1967.) Briefly, the procedure involves ball milling a fine Zn-dust in a varnolene dispersion so as to "flatten" the Zn particles. The residual varnolene is removed by repeated washing with acetone. Characterization data are given in Table 1 and Figure 3.

### IV. Future Program

The selection of samples for the future program will be based on Delco-Remy's electrode evaluations currently in progress.

### V. Appendix

Electron micrographs at 25,200X are shown for the doped ZnO samples and an optical micrograph at 1000X for the flaked Zn-dust.

TABLE 1

Characterization Data for Pb- and Al-doped ZnO and Flaked Zn-dust Samples

Sample No.	243-107-5	243-41-2	243-123-2
Type	Pb-doped ZnO	High Conductivity Al-doped ZnO	Flaked Zn-dust
Particle Size	0.42 $\mu$	1.04 $\mu$	*
Surface Area	3.0 M <sup>2</sup> /G	1.3 M <sup>2</sup> /G	--
Chemical Analysis	0.24% Pb	0.27% Al	0.08% Pb 96.7% Tot. Zn
		0.02% Cl	0.002% Fe 91.5% Met. Zn
Spectrographic Analysis -			
Element			
Zn	vs	vs	vs
Cd	xf	xf	w
Pb	w-m	xf-vf	w
Ca	--	--	vf-f
Fe	xf	xf	vf-f
Si	xf-vf	f	vf-f
B	Trace	Trace	vf-f
Al	vf	w	vf
Cu	xf-vf	xf-vf	xf-vf
Bi	--	--	xf
Mg	xf	xf	xf
Sn	--	--	xf
Mn	--	xf	Trace
Ti	--	--	Trace
Sb	Trace	Trace	Trace

\*Average flake thickness = 2.5 $\mu$





Figure 1. Electron Micrograph of  
Sample 243-107-5 - French Process ZnO + 0.24% Pb  
Calcined 600°C. in Air  
Particle Size = 0.42 $\mu$   
Magnification = 25,200X

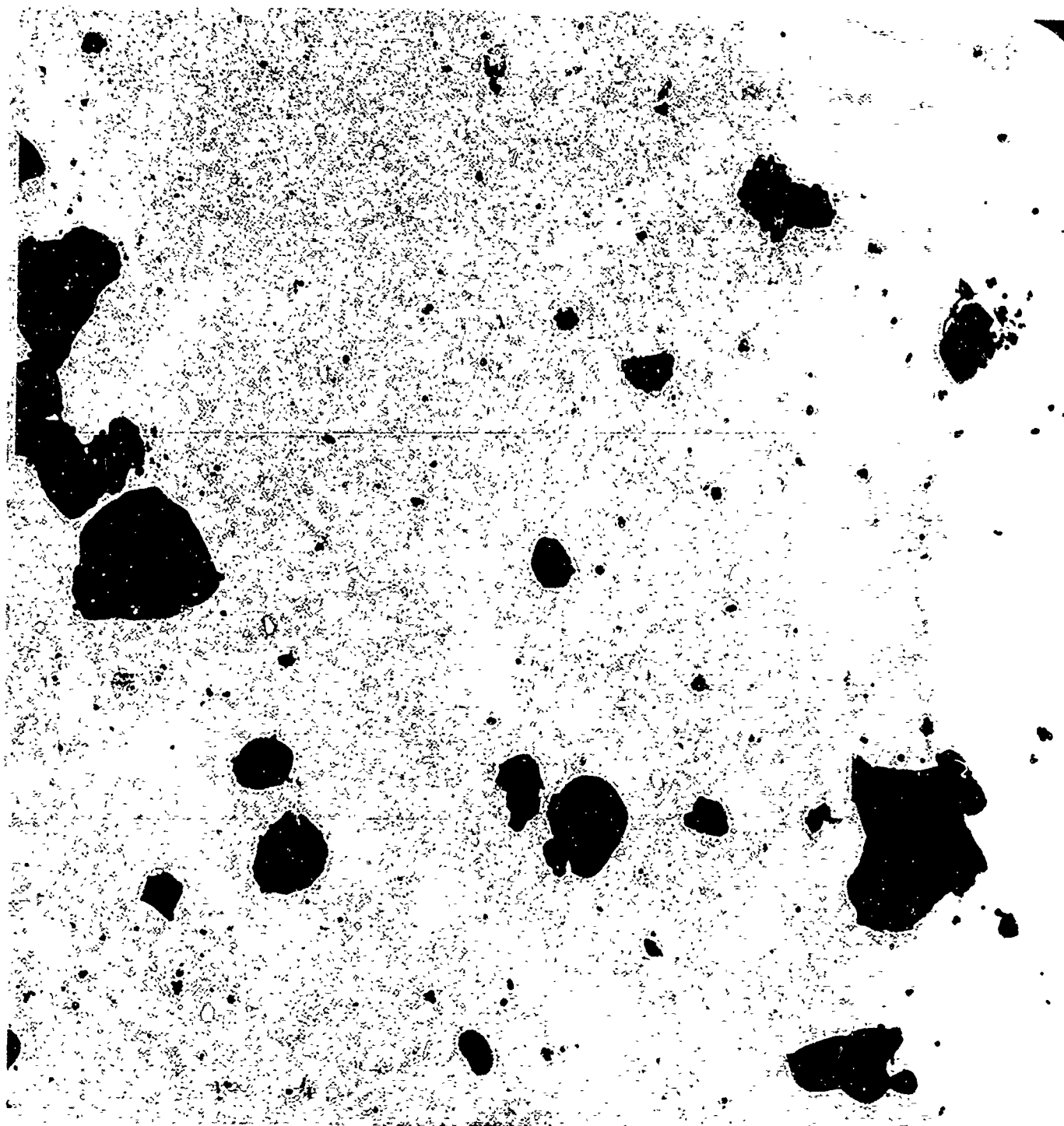


Figure 2. Electron Micrograph of  
Sample 243-41-2 - High Conductivity Al-doped ZnO  
Particle Size =  $1.04\mu$   
Magnification = 25,200X



Figure 3. Optical Micrograph of  
Sample 243-123-2 - Flaked Zn-dust  
Average Flake Thickness =  $2.5\mu$   
Magnification = 1,000X

FINAL REPORT

September 1967 - August 1968

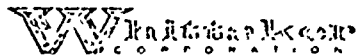
INFLUENCE OF MEMBRANE TRANSPORT  
CHARACTERISTICS ON ELECTROLYTE  
CONCENTRATION AND CONSEQUENT PLATE  
PERFORMANCE

By

A. H. Remanick, M. Shaw and W. I. Nelson

D-R 196419  
Contract No. AF 33(615)3487

Prepared for  
Delco - Remy  
Division of General Motors  
Anderson, Indiana  
46011



NARMCO RESEARCH & DEVELOPMENT DIVISION  
3540 Aero Court • San Diego, California 92123

## TABLE OF CONTENTS

	<u>Page</u>
ABSTRACT	i
SUMMARY	ii
I. INTRODUCTION	1
II. RESULTS	3
A. General	3
1. Definitions	3
2. Plate Conditioning Criteria	5
B. Silver Plates	5
1. Charge Tests	5
2. Discharge Tests	12
C. Cadmium Plates	17
1. Charge Tests	17
2. Discharge Tests	23
D. Zinc Plates	28
1. Charge Tests	28
2. Discharge Tests	37
3. Cycling Effects	42
III. DISCUSSION	49
IV. RECOMMENDATIONS	57
V. REFERENCES	60

# LIST OF TABLES

<u>Table</u>		<u>Page</u>
I.	Silver Plate Charge, 30° C	9
II.	Silver Plate Charge, 0° C	10
III.	Silver Plate Charge, -20° C	11
IV.	Silver Plate Discharge, 30° C	13
V.	Silver Plate Discharge, 0° C	14
VI.	Silver Plate Discharge, -20° C	15
VII.	Cadmium Plate Charge, 30° C	18
VIII.	Cadmium Plate Charge, 0° C	19
IX.	Cadmium Plate Charge, -20° C	20
X.	Cadmium Plate Discharge, 30° C	24
XI.	Cadmium Plate Discharge, 0° C	25
XII.	Cadmium Plate Discharge, -20° C	26
XIII.	Zinc Plate Charge, 30° C	32
XIV.	Zinc Plate Charge, 0° C	33
XV.	Zinc Plate Charge, -20° C	34
XVI.	Zinc Plate Discharge, 30° C	39
XVII.	Zinc Plate Discharge, 0° C	40
XVIII.	Zinc Plate Discharge, -20° C	41

## LIST OF FIGURES

<u>Figure</u>	<u>Page</u>
1. Typical charge curve	6
2. Typical discharge curve	6
3. Effect of KOH concentration on charging cadmium plate at 0° C.	22
4. Effect of KOH concentration on capacity on discharge of cadmium plate at 0° C.	27
5. Effect of temperature on capacity of cadmium plates discharged in 5.0 m KOH.	29
6. Effect of current density on $V_i$ for zinc plates charged at 30° C.	36
7. Effect of concentration on $V_i$ for zinc plates charged at 30° C.	36
8. Effect of temperature on charge acceptance of zinc plates at 60 ma/in <sup>2</sup> .	38
9. Effect of concentration on capacity of zinc plates discharged at 30° C.	43
10. Effect of concentration on capacity of zinc plates discharged at 0° C.	43
11. Effect of current density on capacity of zinc plates discharged at 30° C.	44
12. Effect of current density on capacity of zinc plates discharged at 0° C.	44
13. Effect of temperature on capacity of zinc plates discharged at 60 ma/in <sup>2</sup> .	45
14. Effect of temperature on capacity of zinc plates discharged at 240 ma/in <sup>2</sup> .	45

# LIST OF FIGURES (Cont'd)

<u>Figure</u>		<u>Page</u>
15.	Effect of temperature on capacity of zinc plates discharged at 120 ma/in <sup>2</sup> .	46
16.	Effect of cycle on charge acceptance of zinc plates.	48
17.	Change of anolyte concentration on discharge.	52
18.	Effect of concentration on discharge characteristics.	53
19.	Effect of concentration on voltage.	54
20.	Predicted discharge characteristics - Silver oxide-zinc battery.	56



## ABSTRACT

Charge and discharge characteristics of silver, cadmium, and zinc plates have been investigated in KOH as a function of temperature, current density, and electrolyte concentration. The results were correlated with previous measurements of electrolyte transport in order to determine the effect of design and operational performance on battery characteristics.

## SUMMARY

In order to obtain data for improvement in design of alkaline batteries, a study of the effect of temperature, current density, and electrolyte concentration on silver, cadmium, and zinc plates was performed.

Results of the tests of the silver plates indicated that for both the charge and discharge reactions, plate characteristics were essentially invariant. One exception to this was noted. During charge at high current densities and low temperatures, no charging at the second plateau was noted. Therefore, under certain conditions, the silver plates exhibited a sharp decrease in total capacity.

The cadmium plate charge tests showed a marked effect of current density. This was enhanced by decreasing temperature. Under all conditions, charge acceptance was better at higher KOH concentrations. Results of the discharge tests showed a similar pattern.

In the charge tests of zinc plates, the expected decrease in capacity with increasing current density and decreasing temperature was noted. Increasing KOH caused an abrupt decrease in concentration. During the discharge tests, a maxima in capacity, with respect to concentration, was noted. Although certain trends were evident, it was difficult to separate the effects of the variables studied.

The establishment of typical plate characteristics, under various operational and environmental conditions, formed the second part of a program designed to provide the characteristics of alkaline batteries. Combination of these results with previous derived electrolyte transport data allowed the initial calculation of the expected operation of a typical silver-zinc cell.

## I. INTRODUCTION

Whittaker Corporation is presently engaged in a multiphase program in which it is intended to mathematically describe the various operational and design factors influencing silver-zinc batteries. The overall program is primarily designed to improve low temperature cell operation. It is expected however, that the information derived from these studies will be applicable to battery design and operation at ambient temperatures.

The first phase of the program was designed to elucidate those membrane characteristics which influence electrolyte distribution within the anode and cathode chambers of the cell (Ref. 1). This information formed the basis for mathematical description of change of electrolyte concentration with time, in terms of various operational and design parameters.

The present phase of the program is concerned with the determination of the charge and discharge characteristics of silver, cadmium, and zinc plates with respect to electrolyte concentration and at various temperatures. The effect of current density is also necessarily involved in this study. Although the literature contains certain information of this nature, most of the measurements have been made in complete cells. Since it had been demonstrated in the first phase of the program that membrane parameters markedly influence electrolyte concentration, discharge data based on cells containing membranes could not afford a clear picture of the effect of concentration on discharge characteristics. Furthermore, full cell data involved the discharge characteristics of both plates. In order to derive definite mathematical relationships concerning plate characteristics, separate studies are necessary. These would of course, be combined in the most important phase of the effort which is the description of the overall battery operation.

Even in those cases where literature data is available on single plate studies, the data which is presented in these studies is not readily amenable to mathematical evaluation. It is therefore necessary to establish standard methods in order to obtain meaningful data.

## II. RESULTS

### A. General

#### 1. Definitions

Before detailing the results which have been found to this time, the definitions of the quantities which are to be determined will be discussed.

Although these quantities are routinely used in battery literature, there occasionally appears to be some confusion in their application. For charge tests, the following definitions will be used.

$$\text{Charge acceptance (\%)} = \frac{\text{Total ahr accepted} \times 100}{\text{Total ahr accepted by standard plate}} \quad (1)$$

This definition is used for plates which are electroformed. For those plates which are chemically formed, the following definition should be used.

$$\% \text{ Conversion} = \frac{\text{Total material converted to charged state} \times 100}{\text{Total uncharged material}} \quad (2)$$

It should be noted that the definition of charge acceptance necessarily involves establishment of a standard plate with respect to current density, electrolyte concentration and temperature.

For the discharge tests, the following definition will be used for electro-formed plates:

$$\% \text{ Capacity} = \frac{\text{Total ahr out}}{\text{Total ahr in}} \times 100 \quad (3)$$

In the case of chemically formed plates, the following definitions will be used:

$$\% \text{ Utilization} = \frac{\text{Total ahr out}}{\text{Total theoretical capacity of material}} \times 100 \quad (4)$$

In order to indicate some measure of the voltage characteristics during charge and discharge, we have chosen two quantities,  $V_i$  and percent regulation. For the discharge reaction, these are defined by:

$$V_i = \text{initial stable plateau voltage} \quad (5)$$

$$\% \text{ Regulation (50 mv)} = \frac{\text{ahr out (to 50 mv below } V_i)}{\text{Total ahr out}} \times 100 \quad (6)$$

$$\% \text{ Regulation (100 mv)} = \frac{\text{ahr out (to 100 mv below } V_i)}{\text{Total ahr out}} \times 100 \quad (7)$$

The quantities used for the charge reaction are defined in a similar manner. It should be noted that  $V_i$  does not correspond to the ocv but relates to the first reasonable stable voltage for the charge or discharge. There exists

some arbitrariness in the choice of  $V_i$  for both charge and discharge. However, it was found that small changes in the choice of  $V_i$  did not measurably effect the data. Figures 1 and 2 show the definitive points for the charge and discharge reactions, respectively. The value of the total ahr to cutoff was arbitrarily taken as 1.5 . As will be shown, certain modifications in these definitions will be used for the silver plates. This is due to the two-plateau charge and discharge characteristics of this plate.

## 2. Plate Conditioning Criteria

As previously indicated, descriptions of plate characteristics have been presented. It is difficult, however, to separate the variables studies. In order to alleviate some of these problems, a standard type of plate formation technique was necessary. In this instance, standard refers to a fixed current density, electrolyte concentration, and temperature for the forming cycle. This could readily be accomplished for the silver and cadmium plates, but had to be somewhat modified for the zinc plate. The use of a fixed standard charge and discharge opens the question of what effect an alternate standardization cycle would have on the plate characteristics. Although such information would be of value, in order to accomplish the program within the prescribed limitations, it was necessary to restrict the scope. Additional effort aimed at correlating the effect of cycle procedure on plate performance would undoubtedly be of value.

### B. Silver Plates

#### 1. Charge Tests

In order to establish conditions for preparation of standard silver plates, some preliminary measurements were made. The studies to be described were indicative of some of the results which could be expected during

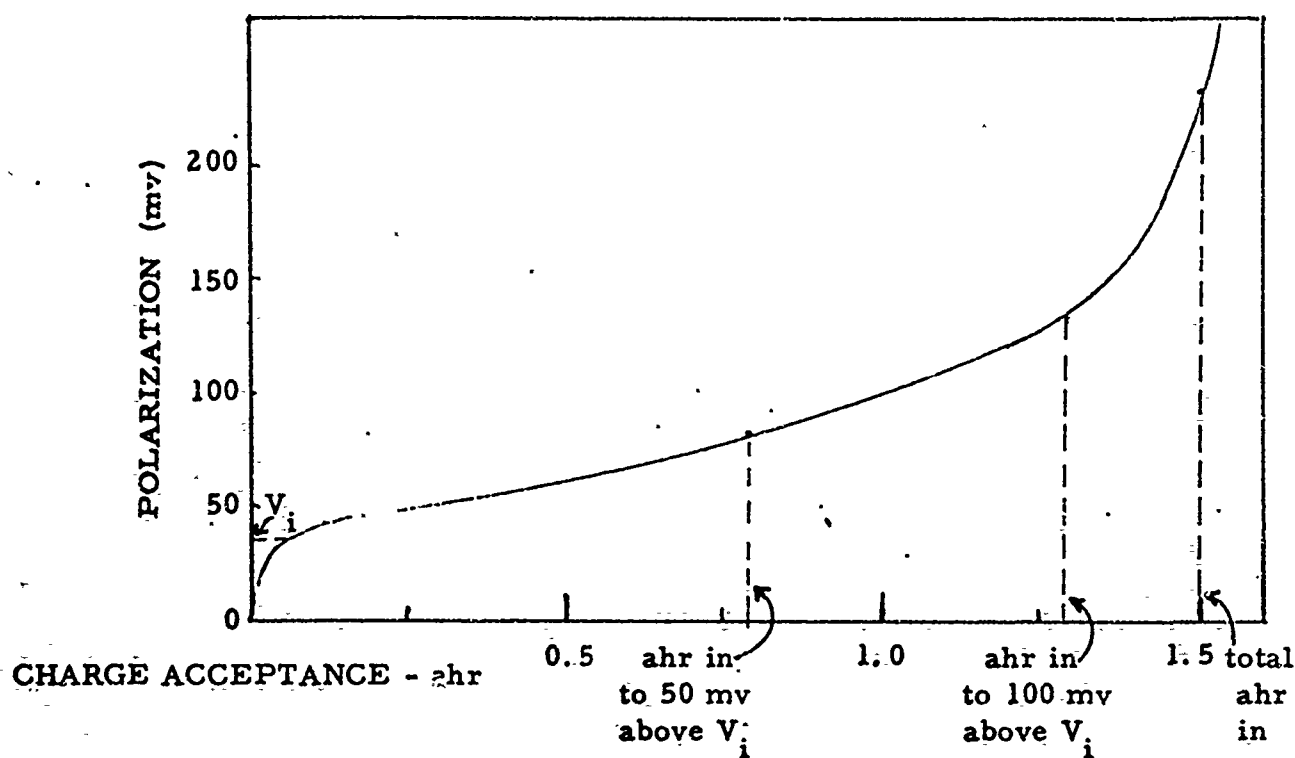


Figure 1. Typical charge curve

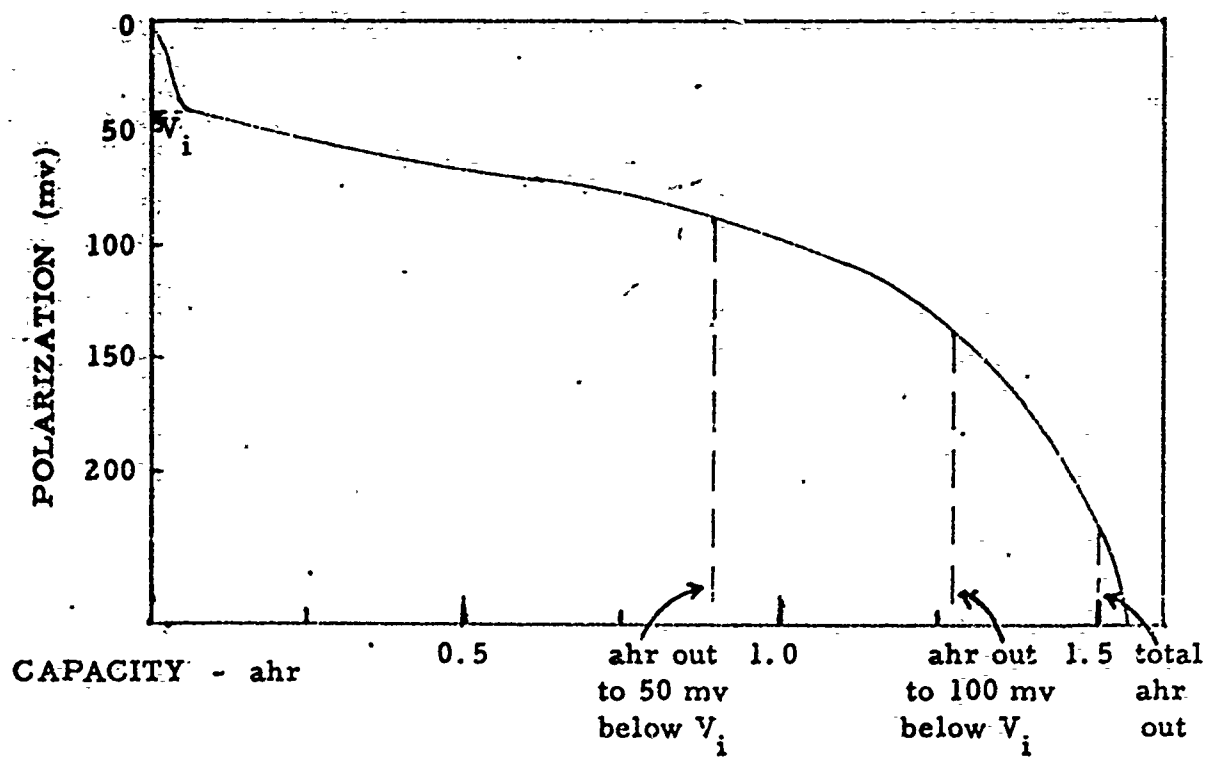


Figure 2. Typical discharge curve



testing of the plates.

Following an initial discharge at  $30 \text{ ma/in}^2$ , the plates were cycled at a charge rate of  $60 \text{ ma/in}^2$ , and at varying discharge rates. A charge rate of  $60 \text{ ma/in}^2$  corresponds to the C/2.5 to C/3 rate. Initial measurements were made against the  $\text{Ag/Ag}_2\text{O}$  reference electrode using nickel counter-electrodes. It soon became apparent there was some instability in the reference electrodes, and these were abandoned.  $\text{Hg/HgO}$  reference electrodes afforded much greater stability. Cells were cycled in an automated system to a charge cutoff voltage of  $0.64 \text{ v}$ , and a discharge voltage of  $0.09 \text{ v}$ , relative to  $\text{Hg/HgO}$ . Duplicate plates were run in cells containing  $\text{KOH}$  at 2.6 m, 8.0 m, and 14.8 m at  $30^\circ \text{C}$ . The major difference between the plates appeared to be a lower charge acceptance at 2.6 m and 14.8 m. Variation between the plates over several charges was about 5%, whereas the difference in capacity between cells at 2.6 m and 8.0 m was about 15%. A similar pattern was shown by the 14.8 m cells. Concentration appeared to have little effect on the capacity, which was essentially 100% for each cell at  $60 \text{ ma/in}^2$ . As expected, there was some decrease of capacity at current densities of  $120 \text{ ma/in}^2$  and  $240 \text{ ma/in}^2$ , however, the loss was only about 10% at the maximum current density. Since the decrease was relatively small, no quantitative measure of the differences in loss as a function of concentration could be made. Electrolyte concentration did not appear to markedly affect the discharge voltage regulation. Each twofold increase of current density caused a decrease of about 10 mv for the voltage on the lower plateau.

The standard plate was prepared as follows: Formed silver plates were discharged to  $0.09 \text{ v}$  vs  $\text{Hg/HgO}$  in 8.0 m  $\text{KOH}$  at  $30^\circ \text{C}$  at  $120 \text{ ma/in}^2$ . They were then charged at  $60 \text{ ma/in}^2$  under the same conditions to a cutoff of  $0.65 \text{ v}$  vs  $\text{Hg/HgO}$ . The discharge-charge cycle was then repeated. Plates showing a variation of 10% between the two charges were discarded.

Plates showing a variation of more than 10% in total charge acceptance from a norm of 1.2 ahr were also not used. Acceptable plates were stored in 8.0 m KOH.

Having established the mode of formation of standard plates, charge tests were carried out at current densities of 30, 60, and 120 ma/in<sup>2</sup> at 30° C, 0° C, and -20° C. KOH concentrations at the two higher temperatures were 2.6, 8.0, 10.6, and 14.9 m, while 5.6, 8.0, 10.6 and 14.9 m KOH were used at -20° C. Duplicate cells were run under all conditions. Results of these tests are presented in Tables I, II, and III.

With the exception of the lack of upper plateau charge acceptance under certain conditions, there appeared to be little effect of concentration on the charging characteristics of the plates. Decreasing temperature appeared to raise the plateau voltages ( $V_1$  and  $V_2$ ) to a small extent, the greatest increase occurring between 30° C and 0° C. Current density did not markedly change the percent acceptance under any of the conditions employed. These results verified the generally accepted description of the silver plate as having non-variant characteristics under a range of conditions.

As indicated above, the most interesting result was the lack of charge acceptance under certain conditions. Other authors have also observed this phenomena during studies concerning the formation of  $Ag_2O_3$  (Ref. 2). This characteristic was manifested under conditions of increasing current density, increasing concentration, and decreasing temperature. These facts imply that there may be an intermediate kinetic step between the reactions corresponding to the two charging steps. Evidently the reaction is dependent upon both current density and electrolyte concentration. Whether this reaction involves physical or chemical changes is not known

TABLE I  
SILVER PLATE CHARGE, 30° C

<u>C.D.<sub>2</sub></u> <u>ma/in</u>	<u>Conc.</u> <u>m</u>	<u>V<sub>1</sub></u> <u>Volts</u>	<u>V<sub>2</sub></u> <u>Volts</u>	<u>L. P.</u> <u>%</u>	<u>Accept.</u> <u>%</u>
30	2.6	0.279	0.554	44.5	106
30	8.0	0.273	0.576	42.3	102
30	10.7	0.273	0.580	46.0	101
30	14.9	0.276	0.580	43.3	102
60	2.6	0.268	0.555	47.5	95.8
60	8.0	0.263	0.549	40.0	97.6
60	10.7	0.261	0.546	37.0	97.3
60	14.9	0.258	0.547	37.6	98.8
120	2.6	0.292	0.576	47.7	89.1
120	8.0	0.280	0.571	42.1	89.5
120	10.7	0.275	0.566	45.1	98.0
120	14.9	0.270	0.566	44.5	92.7

$V_1$  = Stable voltage of lower plateau.

$V_2$  = Stable voltage of upper plateau (usually reached within a few minutes after transition from charging at lower plateau to charging at higher plateau).

$$\% \text{ L. P.} = \frac{\text{ahr in (lower plateau)}}{\text{Total ahr in (test charge)}} \times 100$$

The cutoff point for determining the accepted charge on the lower plateau was the midpoint between the transition from the lower plateau to the upper plateau.

TABLE II  
SILVER PLATE CHARGE, 0° C

<u>C.D. <sup>2</sup> ma/in</u>	<u>Conc. m</u>	<u>V<sub>1</sub> Volts</u>	<u>V<sub>2</sub> Volts</u>	<u>L.P. %</u>	<u>Accept. %</u>
30	2.6	0.339	0.587	48.3	96.4
30	8.0	0.297	0.568	44.1	103
30	10.7	0.307	0.575	44.3	103
30	14.9	0.289	0.579	49.8	101
60	2.6	0.315	0.569	42.9	97.3
60	8.0	0.328	0.588	47.7	86.1
60	10.7	0.310	0.579	46.8	93.4
60	14.9	0.315	0.587	49.8	87.7
120	2.6	0.311	0.560	46.7	89.7
120	8.0	0.329	0.582	42.4	87.6
120	10.7	0.315	0.575	46.0	91.1
120	14.9	0.320	(a)	-	42.3

(a) No charge acceptance at high plateau.

TABLE III

## SILVER PLATE CHARGE, -20° C

<u>C.D.</u> <u>ma/in<sup>2</sup></u>	<u>Conc.</u> <u>m</u>	<u>V<sub>1</sub></u> <u>Volts</u>	<u>V<sub>2</sub></u> <u>Volts</u>	<u>L.P.</u> <u>%</u>	<u>Accept.</u> <u>%</u>
30	5.0	0.326	0.559	42.7	94.6
30	8.0	0.334	0.578	43.8	93.5
30	10.7	0.326	0.575 (b)	46.2	90.5
30	14.3	0.314	(a)	-	35.5
60	5.0	0.335	0.572	40.5	94.5
60	8.0	0.348	0.592	45.2	92.5
60	10.7	0.328	0.577(b)	42.4	88.9
60	14.3	0.331	(a)	-	36.9
120	5.0	0.332	0.562	37.7	94.2
120	8.0	0.363	0.583(b)	35.2	86.2
120	10.7	0.350	(a)	-	31.1
120	14.3	0.353	(a)	-	23.8

(a) No charge acceptance at high plateau.

(b) Only one cell accepted charge at high plateau.

at this time. Dependence on both concentration and current density would, however, seem to indicate that the intermediate step involves a chemical reaction.

Determination of the exact crossover point between acceptance and non-acceptance at the high plateau requires further testing. It will be necessary to evaluate charge acceptance at intermediate concentrations, current densities, and temperatures in order to determine the exact crossover point with respect to each of these variables. On the basis of the present data, it appears that silver plates operating at  $-20^{\circ}\text{C}$  will not accept charge at the high plateau at KOH concentrations of greater than 8.0 m.

## 2. Discharge Tests

Discharge tests were carried out at current densities of 60, 120, and 240  $\text{ma/in}^2$  in 2.6, 8.0, 10.7, and 14.9 m KOH at  $30^{\circ}\text{C}$  and  $0^{\circ}\text{C}$ . At  $-20^{\circ}\text{C}$ , only concentrations of 8.0 and 10.7 m were used because of the possibility of electrolyte freezing. The results of these tests are presented in Tables IV, V, and VI.

$V_1$  did not stabilize until about 10 minutes after initiation of discharge. The divalent plateau was not observed with our plates, probably because of storage. It was observed during preparation of the standard plates, since there was no time delay between charge and discharge. Whether this loss of activity of the higher plateau is due to disproportionation according to reaction 8 or to auto-reduction according to reaction 9 cannot be decided. However, since the capacity did not markedly decrease, it would appear that disproportionation was the primary cause for the absence of the upper voltage plateau.

TABLE IV

## SILVER PLATE DISCHARGE, 30° C

<u>C.D. ma/in<sup>2</sup></u>	<u>Conc. m</u>	<u>V<sub>i</sub> Volts</u>	<u>Regulation* %</u>	<u>Capacity %</u>
60	2.6	0.208	93	96.6
60	8.0	0.224	94	98.8
60	10.7	0.206	92	101.6
60	14.9	0.202	94	103.1
120	2.6	0.197	98	94.6
120	8.0	0.197	96	92.0
120	10.7	0.202	93	99.5
120	14.9	0.200	91	100.6
240	2.6	0.190	95	102.0
240	8.0	0.190	93	95.8
240	10.7	0.188	93	98.2
240	14.6	0.187	91	102.2

\* To 50 mv below V<sub>i</sub>.

TABLE V

## SILVER PLATE DISCHARGE, 0° C

<u>C.D. ma/in<sup>2</sup></u>	<u>Conc. m</u>	<u>V<sub>i</sub> Volts</u>	<u>Regulation* %</u>	<u>Capacity %</u>
60	2.6	0.206	95	93.3
60	8.0	0.186	92	95.2
60	10.7	0.184	91	95.4
60	14.9	0.174	94	94.8
120	2.6	0.198	95	91.2
120	8.0	0.186	95	86.4
120	10.7	0.179	93	94.9
120	14.9	0.175	87	89.0
240	2.6	0.198	95	95.5
240	8.0	0.165	94	91.4
240	10.7	0.183	95	94.4
240	14.9	0.154	89	86.2

\* To 50 mv below V<sub>i</sub>.

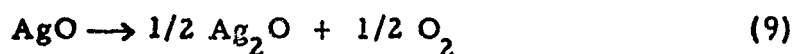


TABLE VI

## SILVER PLATE DISCHARGE, -20° C

<u>C.D. ma/in<sup>2</sup></u>	<u>Conc. m</u>	<u>V<sub>i</sub> Volts</u>	<u>Regulation* %</u>	<u>Capacity %</u>
60	8.0	0.180	97	99
60	10.7	0.162	96	89.5
120	8.0	0.142	96	80.8
120	10.7	0.163	97	89.0
240	8.0	0.147	94	94.3
240	10.7	0.129	95	87.8

\* To 50 mv below V<sub>i</sub>.



Electrolyte concentration has little effect on regulation capacity and  $V_i$  at 30° C. At 0° C, increasing concentration causes a decrease in  $V_i$ , although the trend was not uniform for all current densities. The general decrease of  $V_i$  with concentration does not seem to be due to electrolyte resistivity change, which shows a maximum at about 9.0 m. The effect may be related to electrolyte viscosity changes, since the latter increases with concentration. Further measurements are required to establish this relationship.

Electrolyte concentration does not affect percent regulation to any marked degree at 0° C. No definite conclusions can be made regarding the effect of concentration on capacity, since the differences are not much greater than the usual average deviation (3%) within individual runs. The plates appear to exhibit essentially invariant characteristics at -20° C.

As expected, current density decreases  $V_i$  by about 10 mv for each twofold increase at 30° C. No effect on regulation or capacity was noted at this temperature. Similar results occur at 0° C except for the effect on  $V_i$ . In this instance, there was essentially no difference in  $V_i$  with respect to current density for the 2.6 m and 10.6 m solution. At the two other concentrations,  $V_i$  decreases by about 20 mv on changing from 120 ma/in<sup>2</sup> to 240 ma/in<sup>2</sup>. These trends do not appear to occur in a direct manner, and are sufficiently small so as to be masked by other plate characteristics. In general,  $V_i$  is lowered with increasing current density at -20° C.

Although not uniformly observed, decreasing the temperature from 30° C to -20° C causes a 10% decrease in capacity. This appears to occur at all current densities. Percent regulation remains high at all temperatures.

The effect of temperature is most pronounced on  $V_i$ , this effect being dependent on concentration. At 60 ma/in<sup>2</sup>, an overall decrease of about 40 mv was noted. As stated earlier, the decrease is more marked at higher concentrations. At 120 ma/in<sup>2</sup>, the overall decrease in  $V_i$  is about the same, but the concentration correlation is reversed. That is,  $V_i$  for the 8.0 m cells is lower than  $V_i$  for the 10.7 m cells at -20° C. At 240 ma/in<sup>2</sup> the temperature effect becomes more marked in that the voltage drop becomes greater at the higher concentration.

### C. Cadmium Plates

#### 1. Charge Tests

In order to establish consistent characteristics of the pressed powder plates under standard conditions, it was necessary to charge and discharge the plates for at least ten cycles. Standard conditions consisted of charging at 30 ma/in<sup>2</sup> and discharging at 60 ma/in<sup>2</sup> in 8.0 m KOH at 30° C. Physical integrity of the plates was maintained by the use of a pella wrap covered by a layer of nickel grid material. The charge cutoff voltage was 1.05 v vs Hg-HgO, while the discharge cutoff was 0.75 v. Results of the last two standard cycles were used for test comparisons. Charge tests were carried out at current densities of 15, 30, 60, and 120 ma/in<sup>2</sup>, at temperatures of 30°, 0°, and -20° C. Electrolyte concentrations were 2.5, 5.0, 8.0 and 10.7 m KOH at the two high temperatures, while 5.0, 8.0 and 10.7 m KOH were used at -20° C. Test results are presented in Tables VII, VIII, and IX.

TABLE VII  
CADMIUM PLATE CHARGE, 30° C

<u>C.D. ma/in<sup>2</sup></u>	<u>Conc. m</u>	<u>V<sub>i</sub> Volts</u>	<u>Accept. %</u>
15	2.5	0.925	97.5
15	5.0	0.930	100.0
15	8.0	0.924	101.0
15	10.7	0.922	102.0
30	2.5	0.923	81.8
30	5.0	0.932	86.7
30	8.0	0.926	101.0
30	10.7	0.928	102.0
60	2.5	0.946	82.7
60	5.0	0.944	88.1
60	8.0	0.934	97.4
60	10.7	0.936	97.8
120	2.5	0.962	57.6
120	5.0	0.961	67.3
120	8.0	0.944	81.3
120	10.7	0.945	77.8

TABLE VIII

## CADMIUM PLATE CHARGE, 0° C

<u>C.D. ma/in<sup>2</sup></u>	<u>Conc. m</u>	<u>V<sub>i</sub> Volts</u>	<u>Accept. %</u>
15	2.5	0.952	40.7
15	5.0	0.949	62.4
15	8.0	0.942	78.8
15	10.7	0.934	85.0
30	2.5	0.958	21.2
30	5.0	0.963	41.7
30	8.0	0.951	71.4
30	10.7	0.940	78.9
60	2.5	0.973	7.1
60	5.0	0.976	21.4
60	8.0	0.961	61.5
60	10.7	0.949	70.2
120	2.5	1.007	6.0
120	5.0	0.997	16.1
120	8.0	0.981	45.1
120	10.7	0.962	59.4

TABLE IX

## CADMIUM PLATE CHARGE, -20° C

<u>C.D.</u> <u>ma/in<sup>2</sup></u>	<u>Conc.</u> <u>m</u>	<u>V<sub>i</sub></u> <u>Volts</u>	<u>Accept.</u> <u>%</u>
15	5.0	1.005	1.9
15	8.0	0.987	20.8
15	10.7	0.974	27.8
30	5.0	1.027	0.0
30	8.0	1.016	10.1
30	10.7	0.986	16.3

NOTE: No charge acceptance occurs at 60 and 120 ma/in<sup>2</sup>.

There is a marked decrease in charge acceptance as a function of increasing current density and decreasing temperatures as well as concentration. The most marked effect is that of temperature. This is reflected in complete lack of charge acceptance at  $-20^{\circ}\text{C}$  for current densities of 60 and  $120\text{ ma/in}^2$ .

At  $30^{\circ}\text{C}$ , concentration effects begin to appear immediately after changing current densities from 15 to  $30\text{ ma/in}^2$ . The most pronounced effect occurs between 2.5 and 5.0 m, although the percent acceptance is measurably decreased between 5.0 and 8.0 m. Little difference was noted between current densities of 30 and  $60\text{ ma/in}^2$ . Increasing the current density to  $120\text{ ma/in}^2$  causes a marked decrease at all concentrations. Again, the most noticeable decrease is at 2.5 m KOH.

The results at  $0^{\circ}\text{C}$  resemble those at  $30^{\circ}\text{C}$ , in that a marked decrease in charge acceptance occurs at 2.5 m KOH. In addition, increasing the current density causes an almost complete loss of acceptance at 2.5 m KOH.

At  $-20^{\circ}\text{C}$ , the effect of current density is considerably more pronounced. No charge acceptance occurs at all at 60 or  $120\text{ ma/in}^2$ . At 15 or  $30\text{ ma/in}^2$ , the total capacity is essentially zero in 5.0 m KOH, while a marked decrease in capacity occurs at 8.0 m and 10.7 m KOH. Typical results are presented in Figure 3.

We have not detailed the percent regulation of the cadmium plates, as previously defined, since in all cases, the voltage rise during the major portion of the charge test was relatively low. In all cases, percent regulation on charge was at least 85%.

As stated previously, charge acceptance was terminated 150 mv above ocv.

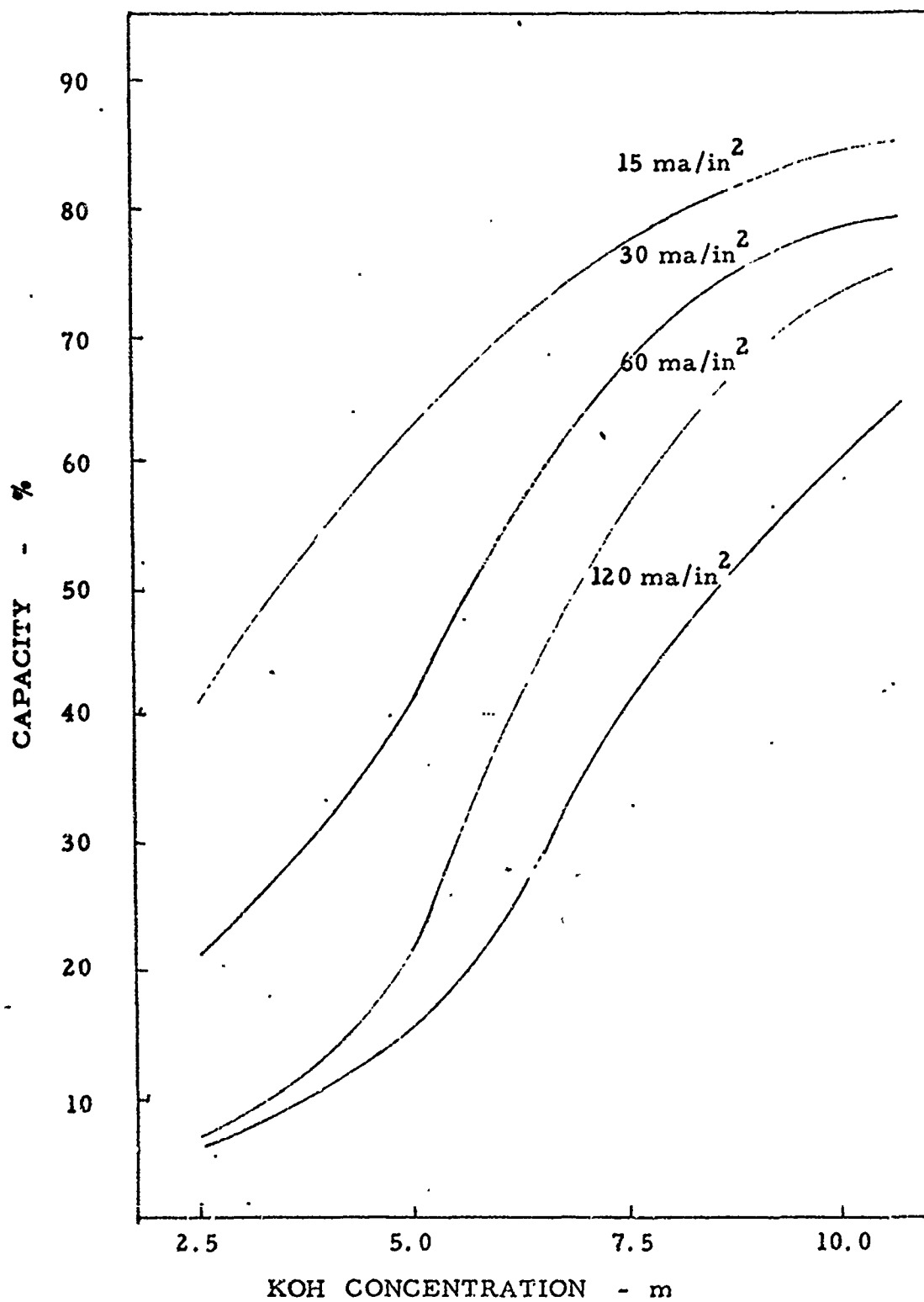


Figure 3. Effect of KOH concentration on charging cadmium plate at 0° C.



This value was chosen since it represented an inflection point in the charge curve. In some of the tests at low temperature, charging was allowed to rise above this point, since the acceptance to 150 mv above ocv was rather brief. As expected, mixed potential due to both the plate reaction and oxygen evolution was observed. This potential was not fixed, and rose during the measurements from 1.3 v to 1.6 v (vs Hg-HgO). Although some charging of the cadmium plates occurred, the total acceptance was rather erratic under these conditions.

## 2. Discharge Tests

After preparation of standard plates in the same manner as the charge tests, discharge tests were run at 60, 120, 180, and 240 ma/in<sup>2</sup> in 2.5, 5.0, 8.0, and 10.7 m KOH at 30° C and 0° C. At -20° C, only concentrations of 5.0, 8.0, and 10.7 m KOH were used. The results of these tests are shown in Tables X, XI, and XII.

The effect of concentration on the capacity was very marked under all conditions investigated. It was interesting to note that the major change occurred between 2.5 m and 5.0 m at temperatures of 30° C and 0° C. At -20° C, the greatest change occurred between 5.0 m and 8.0 m. At this temperature there was also a small decrease in capacity as the concentration changed from 8.0 to 10.7 m. The effect of concentration on capacity at 0° C is illustrated in Figure 4.

Increase of current density caused a decrease in capacity under all conditions. The effect was most severe at 0° C and at the lowest concentration. The effect of current density was not uniform throughout the conditions studied, in that the variation of capacity with current density depended upon

TABLE X. CADMIUM PLATE DISCHARGE, 30° C

<u>C. D.</u> <u>ma/in<sup>2</sup></u>	<u>Conc.</u> <u>m</u>	<u>V<sub>i</sub></u> <u>Volts</u>	<u>Regulation*</u> <u>%</u>	<u>Capacity</u> <u>%</u>
60	2.5	0.881	90.8	78.7
60	5.0	0.893	89.4	95.9
60	8.0	0.901	90.5	99.4
60	10.7	0.895	90.5	101
120	2.5	0.881	87.9	57.3
120	5.0	0.888	82.9	81.1
120	8.0	0.895	84.9	88.2
120	10.7	0.893	86.2	90.7
180	2.5	0.880	82.5	37.0
180	5.0	0.881	68.4	62.3
180	8.0	0.883	81.8	69.4
180	10.7	0.886	78.5	71.8
240	2.5	0.860	63.7	31.9
240	5.0	0.880	68.2	55.2
240	8.0	0.883	75.4	70.7
240	10.7	0.886	70.7	72.0

\* To 50 mv below V<sub>i</sub>.

TABLE XI. CADMIUM PLATE DISCHARGE, 0° C

<u>C. D. ma/in<sup>2</sup></u>	<u>Conc. m</u>	<u>V<sub>i</sub> Volts</u>	<u>Regulation * %</u>	<u>Capacity %</u>
60	2.5	0.876	89.0	61.1
60	5.0	0.885	75.8	83.7
60	8.0	0.893	79.0	84.4
60	10.7	0.898	68.5	88.7
120	2.5	0.873	80.0	38.3
120	5.0	0.879	70.2	63.8
120	8.0	0.887	68.1	61.7
120	10.7	0.889	67.0	66.9
180	2.5	0.865	80.3	24.3
180	5.0	0.865	67.0	46.0
180	8.0	0.879	74.8	46.0
180	10.7	0.882	65.5	53.5
240	2.5	0.848	80.3	15.2
240	5.0	0.848	71.4	33.5
240	8.0	0.870	80.5	37.9
240	10.7	0.870	82.8	40.8

\* To 50 mv below V<sub>i</sub>.

TABLE XII. CADMIUM PLATE DISCHARGE, -20°C

<u>C. D.</u> <u>ma/in<sup>2</sup></u>	<u>Conc.</u> <u>m</u>	<u>V<sub>i</sub></u> <u>Volts</u>	<u>Regulation*</u> <u>%</u>	<u>Capacity</u> <u>%</u>
60	5.0	0.853	87.1	30.3
60	8.0	0.892	89.8	56.1
60	10.7	0.869	80.6	45.8
120	5.0	0.843	79.5	16.8
120	8.0	0.864	79.8	38.9
120	10.7	0.867	76.9	32.4
180	5.0	0.820	82.8	8.8
180	8.0	0.845	81.7	22.2
180	10.7	0.840	82.8	23.5
240	5.0	0.827	83.7	9.7
240	8.0	0.838	80.4	20.9
240	10.7	0.832	80.1	16.5

\* To 50 mv below V<sub>i</sub>

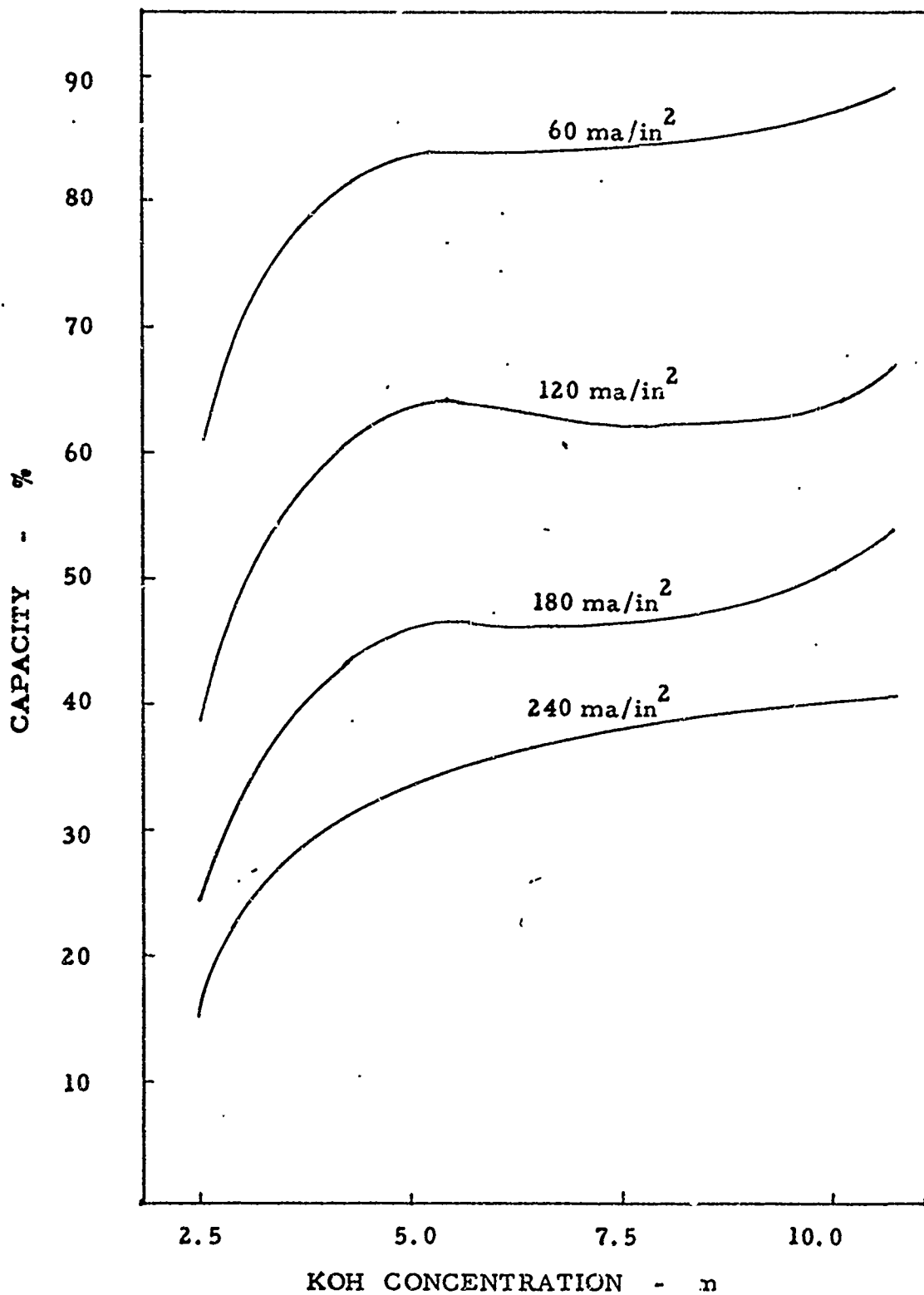


Figure 4. Effect of KOH concentration on capacity on discharge of cadmium plate at 0° C.

both concentration and temperature. As with most of the data, changes in plate characteristics were not a simple function of any single variable.

The effect of temperature on plate capacity was quite pronounced, the largest variation appearing between 0° C and -20° C. This is shown in Figure 5 for an electrolyte concentration of 5.0 m. Here again, it was difficult to relate the effect of any single variable on plate capacity, since the change was not entirely uniform.

The greatest effects of concentration, temperature, and current density were noted in the plate capacity. There appeared to be relatively minor effects on the percent regulation, which did not display any definite trend.

$V_i$  suffered a 10-20 mv change as the concentration was changed from 2.5 m to 5.0 m at 30° and 0° C. This was also shown at -20° C between 5.0 and 8.0 m. The effect of current density is slight, and only at 0° C and -20° C. Similarly, decreasing temperature causes a small decrease in  $V_i$ . The overall effect of both these variables is relatively small since the greatest decrease shown in  $V_i$  is only 90 mv lower than the ocv.

#### D. Zinc Plates

##### 1. Charge Tests

As anticipated, study of the electrolyte concentration effect on zinc electrode characteristics did not proceed as easily as the corresponding silver and cadmium plate studies. This was due to the high solubility of zincate ion in alkaline electrolyte. The attendant reduction of zincate at the counter-electrode would invalidate any data thereby derived. Furthermore, the physical relationship of the zinc plate in an open test cell is sufficiently different from that in a silver-zinc battery, so as to invalidate any plate

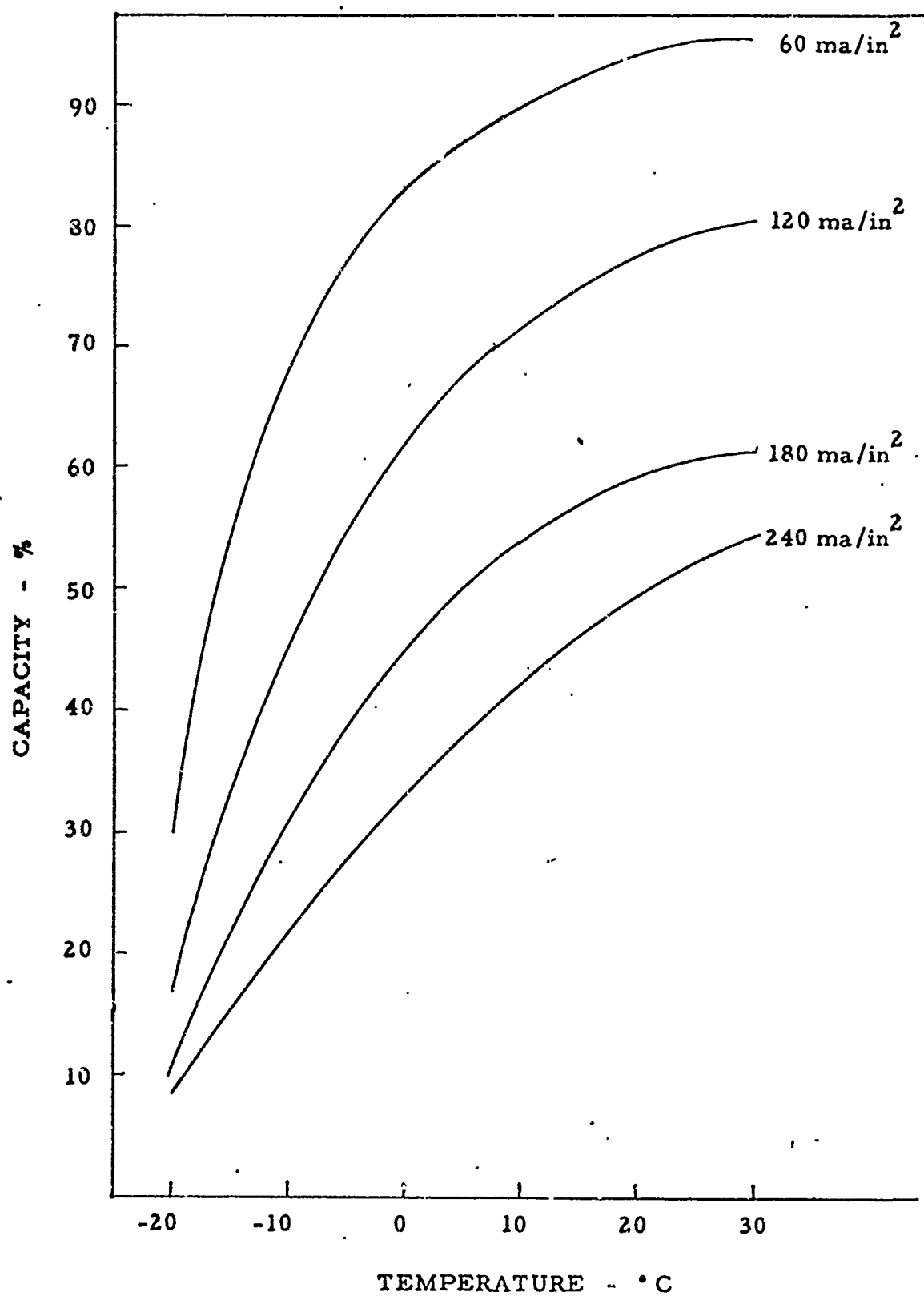


Figure 5. Effect of temperature on capacity of cadmium plates discharged in 5.0 m KOH.

evaluation by this method. On the other hand, it has been demonstrated that in the tightly wrapped configuration of a typical battery, there is a definite configuration in which excess electrolyte would be available for the test cell, and yet provide a method for providing sufficient plate integrity. The plate was therefore wrapped with two types of separators. The first wrap was a polypropylene felt. Use of this material was not expected to inhibit electrolyte diffusion because of the essentially macroscopic pores in the material. Furthermore, the relatively large void volume provided excess electrolyte. Several layers of Visking V-7 membrane were then wrapped around the plate. The entire plate stack was placed in the test cell under slight compression.

Although the membrane will absorb electrolyte, resulting in a change of initial concentration because of the ratio of membrane to electrolyte used, this is generally less than one half unit in molality. The problem of zincate diffusion and absorption by the membrane must also be considered. The absence of zinc deposition at the counterelectrode indicates that sufficient membrane is available to stop zincate diffusion. Furthermore, the charge-discharge characteristics of the plates are reasonably uniform under a standard charge-discharge regimen. It appears, therefore, that zincate absorption does not markedly alter the plate characteristics. Physical examination of the cell pack after a few cycles has indicated that the described methods apparently maintain sufficient plate integrity for the few cycles necessary for each plate standardization and test. Since initial testing indicated a marked difference between plates, four plates were tested under each set of experimental conditions.

A standard formation procedure consisted of discharge at  $60 \text{ ma/in}^2$  followed by three charge-discharge cycles at the same current density. Formation was accomplished at  $30^\circ \text{ C}$ . The charge cutoff was  $1.65 \text{ v}$  vs



Hg - HgO while the discharge cutoff was 1.10 v vs Hg - HgO.

The concentration of electrolyte used for the plate formation was the same as that used in the tests. This is in contrast to the procedure used for the silver and cadmium plates, which were formed in 8.0 m KOH and then tested in the appropriate electrolyte. The physical condition of the plate after formation did not allow removal of the original electrolyte. Sufficient electrolyte was present in the cell to negate changes of concentration due to hydrogen and oxygen removal at the counterelectrode during the charge-discharge cycle.

Charge tests were run at 60, 120, and 240 ma/in<sup>2</sup> at 30° C and 0° C for concentrations of 2.5, 5.0, 8.0, and 10.7 m KOH. At -20° C, only concentrations of 5.0, 8.0, and 10.7 m were employed at the indicated current densities. Results of these tests are presented in Tables XIII, XIV, and XV.

The zinc plates exhibited about a thirty percent variation in total capacity. This was not unexpected for pressed powder zinc plates. Some plates exhibited characteristics quite different from those within a certain test group. This usually occurred with plates having a lower capacity. Data obtained from these plates was disregarded if it differed significantly from that obtained from the other plates within the test run. Even with those plates having reasonably similar nominal capacities, some data scatter was evident, particularly at the higher current densities. Percent capacity variation was usually within 10%, although variation in percent regulation sometimes exceeded this value. Data was not used in those cases where the regulation differed markedly from that of other plates within the test group.

In all cases, there was a decrease in charge acceptance with each cycle. Therefore, in order to determine the relative acceptance of the plates under

TABLE XIII  
ZINC PLATE CHARGE, 30° C

<u>C.D. <sub>2</sub></u> <u>ma/in</u>	<u>Conc.</u> <u>m</u>	<u>V<sub>i</sub></u> <u>Volts</u>	<u>Regulation*</u> <u>%</u>	<u>Regulation**</u> <u>%</u>	<u>Accept.</u> <u>%</u>
30	2.5	1.385	84	94	110.0
30	5.0	1.403	78	94	107.0
30	8.0	1.413	80	94	123.0
30	10.7	1.424	84	94	109.0
60	2.5	1.403	72	89	100.0
60	5.0	1.408	73	88	100.0
60	8.0	1.421	69	86	100.0
60	10.7	1.428	71	87	100.0
120	2.5	1.460	69	90	92.7
120	5.0	1.466	64	84	92.0
120	8.0	1.486	67	87	89.6
120	10.7	1.503	68	88	88.5

\* To 50 mv below V<sub>i</sub>.

\*\* To 100 mv below V<sub>i</sub>.

TABLE XIV

## ZINC PLATE CHARGE, 0° C

C.D. ma/in <sup>2</sup>	Conc. m	V <sub>i</sub> Volts	Regulation* %	Regulation** %	Accept. %
30	2.5	1.404	65	83	99.1
30	5.0	1.408	58	81	97.7
30	8.0	1.438	63	85	104.0
30	10.7	1.450	62	79	97.7
60	2.5	1.441	79	90	94.5
60	5.0	1.456	67	80	91.7
60	8.0	1.503	75	93	88.7
60	10.7	1.514	65	88	84.9
120	2.5	1.496	65	86	82.1
120	5.0	1.525	69	90	80.8
120	8.0	1.565	62	-	55.4
120	10.7	(a)	-	-	-

\* To 50 mv below V<sub>i</sub>

\*\* To 100 mv below V<sub>i</sub>

NOTE: All cells reached cutoff within 2 minutes after start of charge.

TABLE XV

ZINC PLATE CHARGE,  $-20^{\circ}\text{C}$ 

<u>C.D. <sub>2</sub></u> <u>ma/in</u>	<u>Conc.</u> <u>m</u>	<u>V<sub>i</sub></u> <u>Volts</u>	<u>Regulation*</u> <u>%</u>	<u>Regulation**</u> <u>%</u>	<u>Accept.</u> <u>%</u>
30	5.0	1.490	75	91	92.0
30	8.0	1.522	62	88	79.0
30	10.7	1.604	-	-	53.2
60	5.0	1.538	83	96	63.9
60	8.0	1.557	(a)	-	25.6
60	10.7	(b)	-	-	-
120	5.0	1.640	-	-	29.1
120	8.0	(b)	-	-	-
120	10.7	(b)	-	-	-

\* To 50 mv below V<sub>i</sub>

\*\* To 100 mv below V<sub>i</sub>

## NOTES:

(a) Most of charge occurred at about 1.65 v.

(b) All cells reached cutoff within 2 minutes after start of charge.

the test conditions, it was necessary to use an extrapolated value of the expected charge acceptance under standard conditions. This extrapolation technique was verified by maintaining the standard charge-discharge cycle beyond the number of cycles used in the formation. A fairly linear decrease in charge acceptance occurred through the sixth cycle. Test runs were usually the fourth or fifth charge.

Since it was necessary to carry out the plate formation standardization in the same concentration as used for the tests, it may be argued that the discharge tests may not only reflect changes due to the test variations, but also variations due to concentration of the forming electrolyte. However, the similarity of the discharge data obtained at  $60 \text{ ma/in}^2$  at  $30^\circ \text{C}$ , implies that concentration does not alter the discharge characteristics. This does not imply that the charge characteristics are independent of concentration, but does indicate that under the conditions employed ( $60 \text{ ma/in}^2$ ,  $30^\circ \text{C}$ ), little effect is expected. At  $30^\circ \text{C}$ , there is about a 10% change in acceptance with each twofold change in current density. Little effect of concentration is noted except for the increase in  $V_i$ . Current density appears to alter  $V_i$  to a greater extent than concentration. This is shown in Figures 6 and 7.

At  $0^\circ \text{C}$ ,  $V_i$  shows an increase at all current densities and concentrations in a manner similar to that shown at  $30^\circ \text{C}$ . At 60 and  $120 \text{ ma/in}^2$ , only relatively small changes in acceptance are noted. At  $120 \text{ ma/in}^2$ , a very marked change in acceptance is seen. This change is quite concentration-dependent in that at 10.7 m, the plates polarized immediately at the start of the test while at 2.5 and 5.0 m, only a small decrease in acceptance is noted. At 8.0 m, a large decrease in acceptance was shown. This trend was enhanced by a temperature decrease. At  $-20^\circ \text{C}$ , little or no acceptance was evidenced at  $120 \text{ ma/in}^2$  while at  $30 \text{ ma/in}^2$  in 5.0 m KOH, there was little loss of acceptance. The effect of temperature on acceptance is

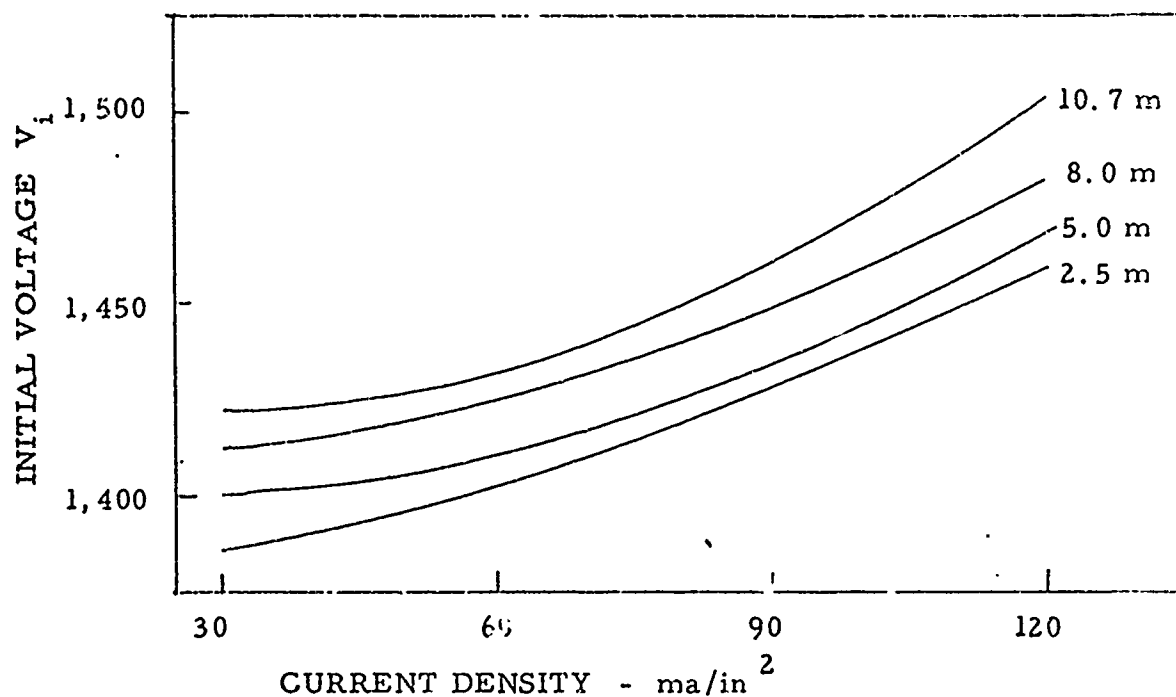


Figure 6. Effect of current density on  $V_i$  for zinc plates charged at 30° C.

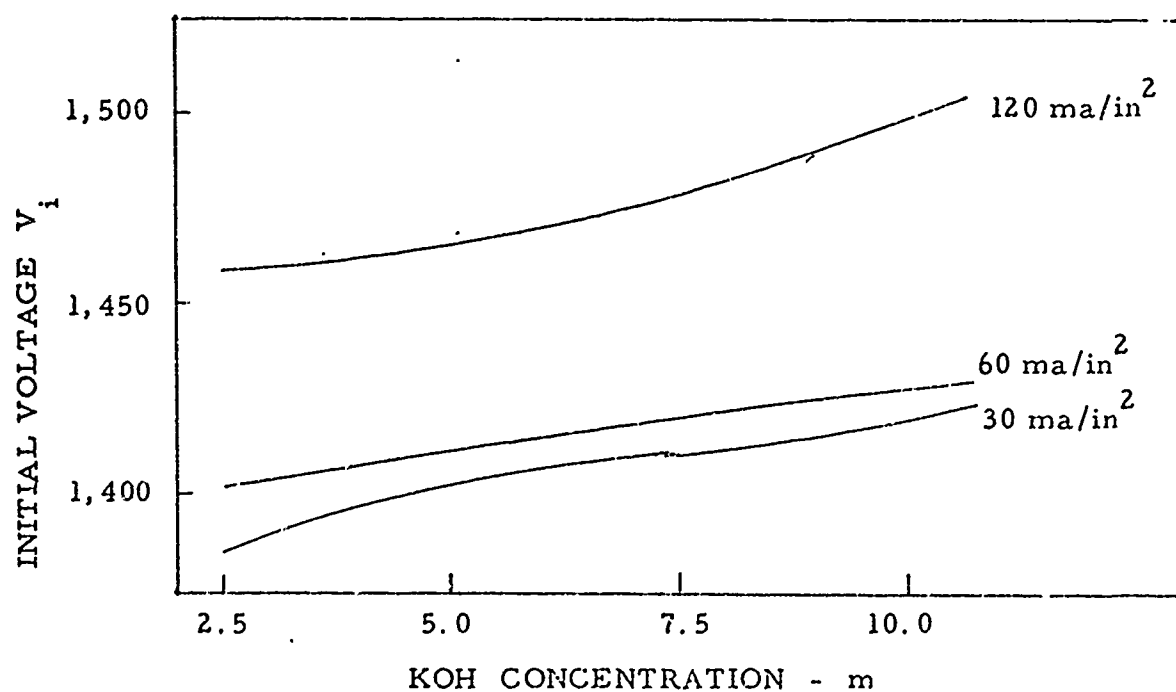


Figure 7. Effect of concentration on  $V_i$  for zinc plates charged at 30° C.

shown in Figure 8, for 60 ma/in<sup>2</sup>. This rather sharp change in polarization characteristics of zinc plates has been noted previously. In the present work we have endeavored to more critically define the areas in which a zinc plate may be used for secondary application.

## 2. Discharge Tests

In contrast to discharge of silver and cadmium plates, the discharge curves for the zinc plates exhibit a greater slope, necessitating a lower cutoff voltage. Also, in order to more adequately describe the shape of the discharge curve, it was necessary to determine the percent regulation at both 50 mv and 100 mv below the initial voltage. The lack of a stable plateau also necessitated a more arbitrary choice of the initial voltage. This was usually chosen at a point where the initial slope became constant.

Plates were conditioned in the same manner as that described for the charge tests except for an additional half-cycle charge. Tests were accomplished at 60, 120, and 240 ma/in<sup>2</sup> in 2.0, 5.0, 8.0, and 10.7 m KOH at 30° C and 0° C. At -20° C, only the latter three molalities were employed. The results of these tests are presented in Tables XVI, XVII, and XVIII.

Results at 30° C indicate that there is an apparent maximum in percent capacity at 5.0 m KOH. As shown in Figure 9, this is not evidenced at 60 ma/in<sup>2</sup>, but only appears at 120 and 240 ma/in<sup>2</sup>. Better regulation is obtained at the lower concentrations, although this may be partially due to the fact that the initial voltage loss is greater at the lower concentrations, such that a flatter discharge from a lower initial voltage is indicated. Although still prevalent, this effect is not as significant for the percent regulation at 100 mv below  $V_i$ .

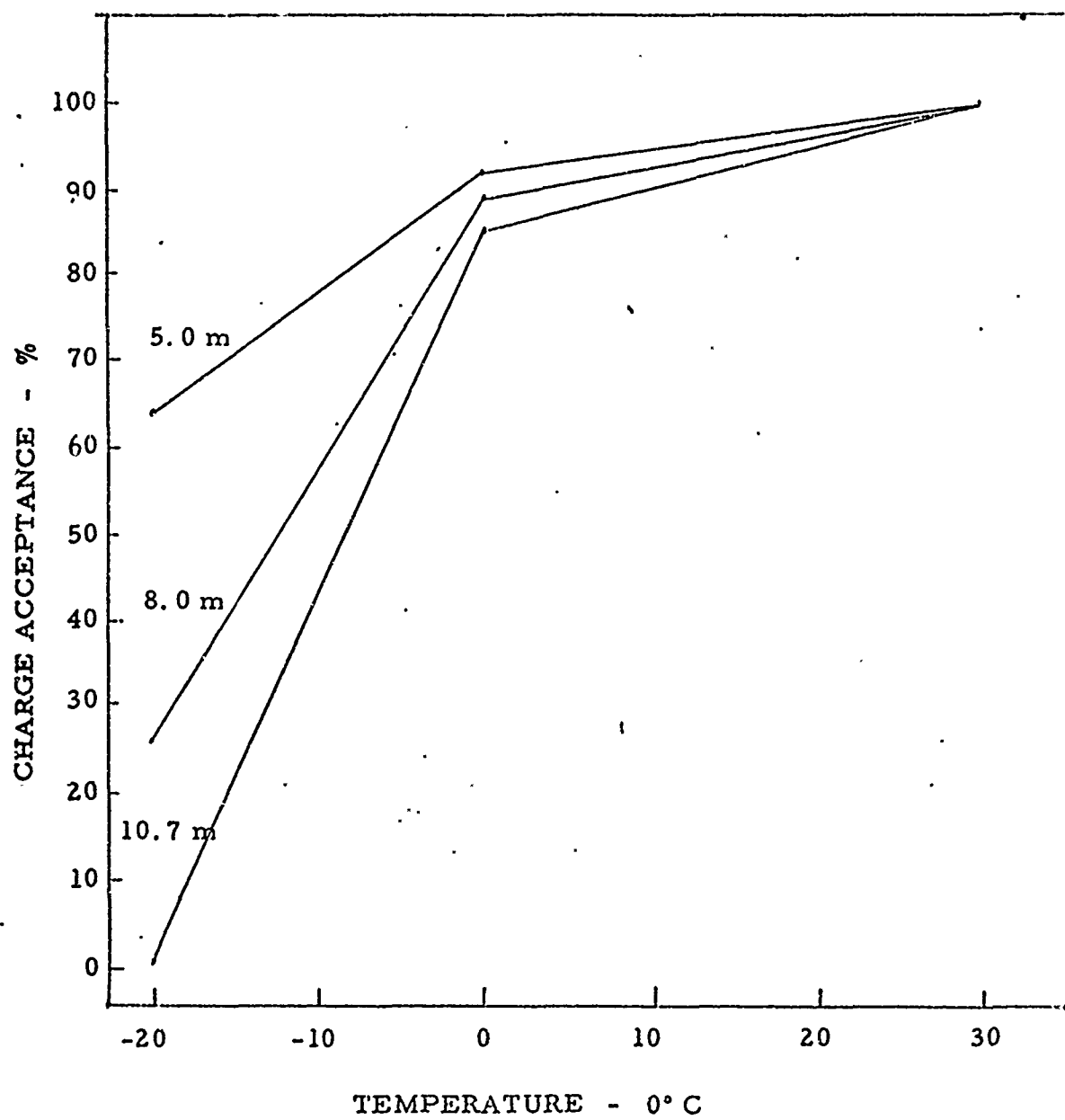


Figure 8. Effect of temperature on charge acceptance of zinc plates at 60 ma/in<sup>2</sup>.



TABLE XVI  
ZINC PLATE DISCHARGE, 30° C

<u>C.D. ma/in<sup>2</sup></u>	<u>Conc. m</u>	<u>V<sub>i</sub> Volts</u>	<u>Regulation* %</u>	<u>Regulation** %</u>	<u>Capacity %</u>
60	2.5	1.275	49	75	96.9
60	5.0	1.318	22	79	94.9
60	8.0	1.336	18	62	92.4
60	10.7	1.345	22	41	90.9
120	2.5	1.266	71	95	61.5
120	5.0	1.270	36	75	82.3
120	8.0	1.286	22	50	68.3
120	10.7	1.279	25	54	76.4
240	2.5	1.200	56	96	35.1
240	5.0	1.212	62	95	49.6
240	8.0	1.260	53	69	38.3
240	10.7	1.232	65	88	40.3

\* To 50 mv below V<sub>i</sub>

\*\* To 100 mv below V<sub>i</sub>

TABLE XVII  
ZINC PLATE DISCHARGE, 0° C

<u>C.D.</u> <u>ma/in<sup>2</sup></u>	<u>Conc.</u> <u>m</u>	<u>V<sub>i</sub></u> <u>Volts</u>	<u>Regulation*</u> <u>%</u>	<u>Regulation **</u> <u>%</u>	<u>Capacity</u> <u>%</u>
60	2.5	1.243	74	92	46.0
60	5.0	1.278	24	77	76.9
60	8.0	1.278	27	46	56.0
60	10.7	1.287	47	64	47.5
120	2.5	1.251	50	84	9.0
120	5.0	1.250	30	68	33.9
120	8.0	1.267	40	67	28.2
120	10.7	1.273	29	59	23.3
240	2.5	1.151	93	(a)	2.8
240	5.0	1.210	51	92	13.3
240	8.0	1.201	51	85	11.6
240	10.7	1.180	65	(a)	6.3

\* To 50 mv below V<sub>i</sub>

\*\* To 100 mv below V<sub>i</sub>

NOTE: (a) V<sub>i</sub> too low to measure 100 mv decrease before cutoff.

TABLE XVIII  
ZINC PLATE DISCHARGE, -20° C

<u>C.D. <sup>2</sup> ma/in</u>	<u>Conc. m</u>	<u>V<sub>i</sub> Volts</u>	<u>Regulation* %</u>	<u>Regulation** %</u>	<u>Capacity %</u>
60	5.0	1.266	33	52	28.9
60	8.0	1.241	28	51	27.8
60	10.7	1.238	28	43	22.2
120	5.0	1.236	31	52	17.0
120	8.0	1.226	26	54	18.9
120	10.7	1.138	32	69	10.8
240	5.0	1.080	50	(a)	5.5
240	8.0	1.065	69	(a)	3.2
240	10.7	-	-	-	(b)

\* To 50 mv below V<sub>i</sub>

\*\* To 100 mv below V<sub>i</sub>

NOTES: (a) V<sub>i</sub> too low to measure 100 mv decrease before cutoff.  
(b) Less than 1% capacity under test conditions.

Comparison of the results at 0° C indicates a decrease of capacity under all conditions, the decrease being dependent on temperature and current density. From Figure 10, it is readily seen that a maximum in percent capacity is present. However, at this temperature, the maximum is most pronounced at 60 ma/in<sup>2</sup> as opposed to the results at 30° C. The change of  $V_i$  is relatively uniform under all conditions, although the variation in regulation appears not to follow the pattern shown at 30° C. It is not unlikely that this is an artifact of changes in initial voltage.

Capacity is quite dependent on current density at all temperatures (see Figures 9 - 12). This is most evident at 30° C where the plates exhibit their greater capacity at this temperature. The effect of temperature, (Figures 13 - 15) is apparently related to both concentration and current density. Although a generally linear decrease in capacity with temperature is noted, the exact shape of the curve is dependent on both of the indicated factors.

### 3. Cycling Effects

As previously noted, we have chosen the best conditions and data presentation in a manner which showed relative plate characteristics. This was done in order to avoid plate to plate variation as much as possible. Since this was not possible for the zinc plates, it was necessary to run a large number of plates in this series. In addition to a lack of uniformity in coulombic capacity, there was a marked effect of concentration on the acceptance as determined from the standardization runs. This is shown in Figure 16. The charge acceptance of the first cycle is taken as a 100%, and subsequent values are based on this cycle. All data represents the average of 20 - 40 determinations. Since our test procedure involved a large amount of electrolyte, the decrease in capacity may have been due

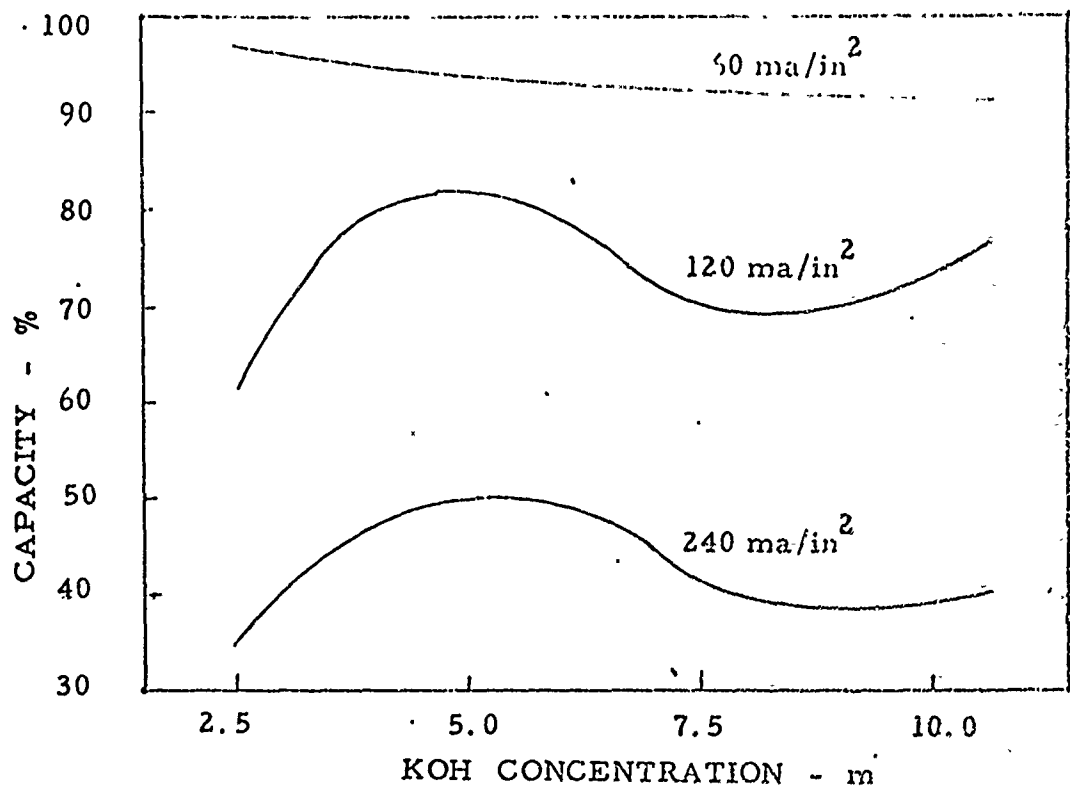


Figure 9. Effect of concentration on capacity of zinc plates discharged at 30° C.

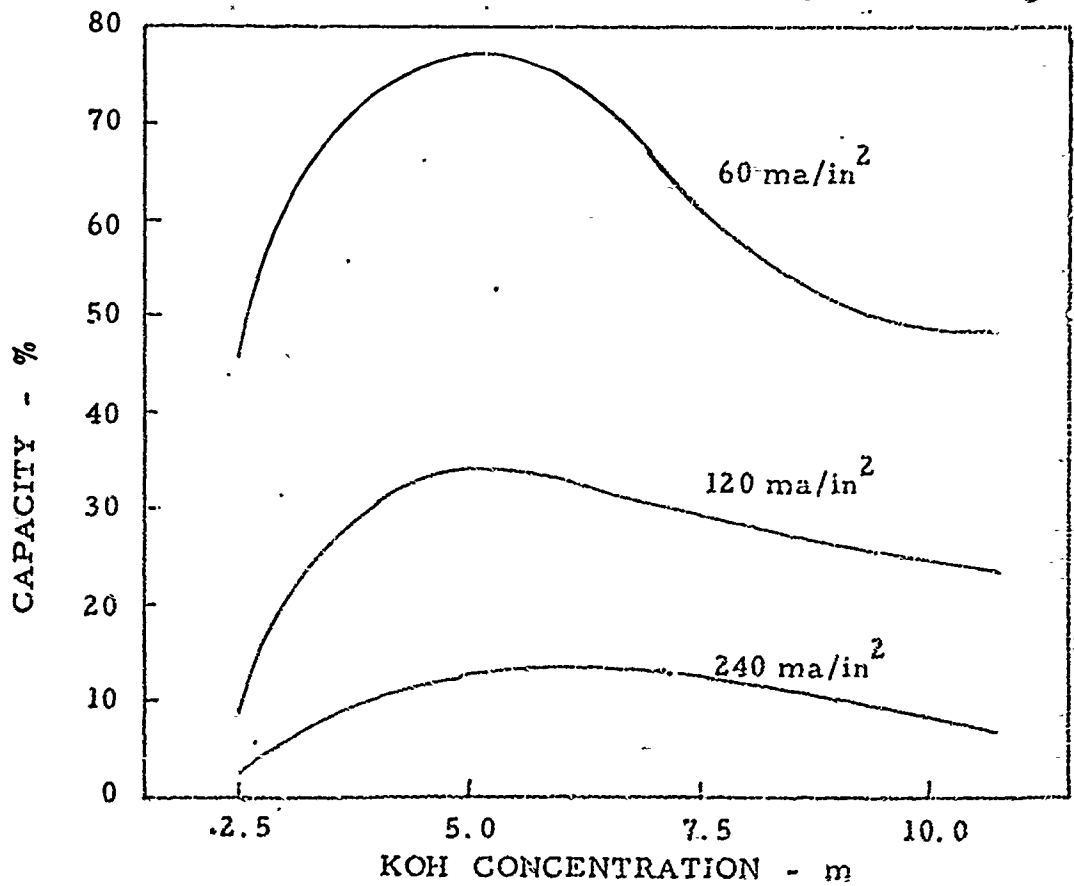


Figure 10. Effect of concentration on capacity of zinc plates discharged at 0° C.

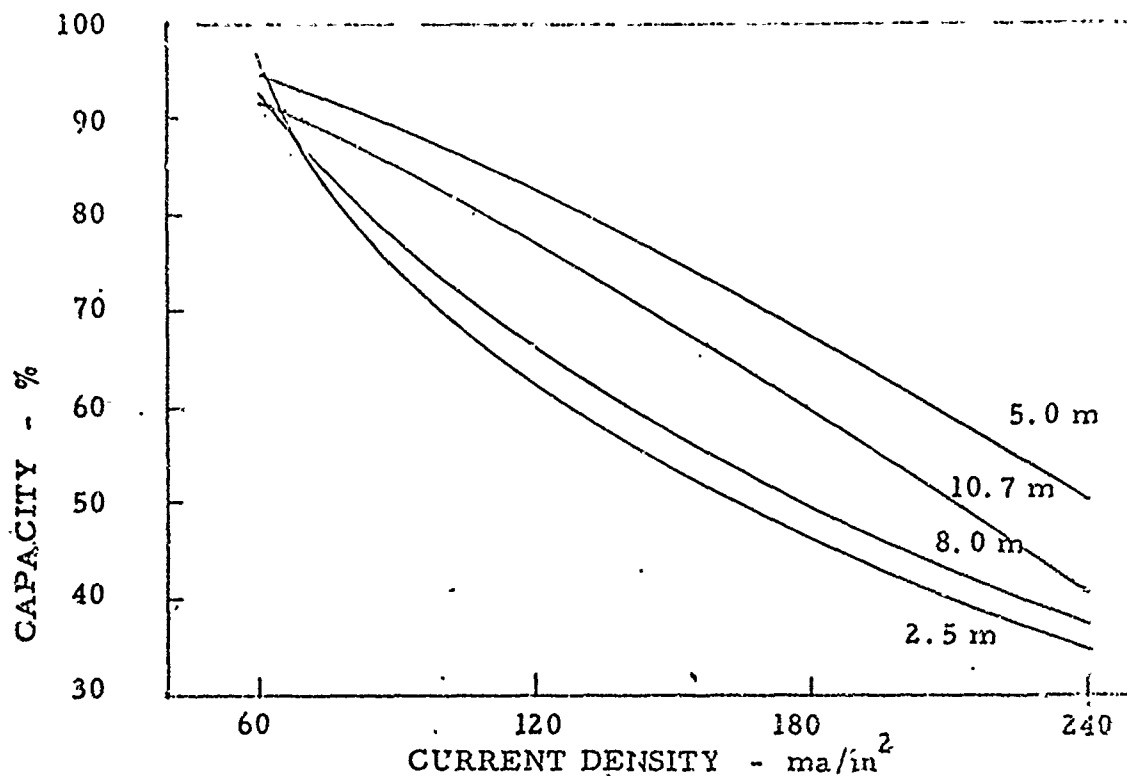


Figure 11. Effect of current density on capacity of zinc plates discharged at 30°

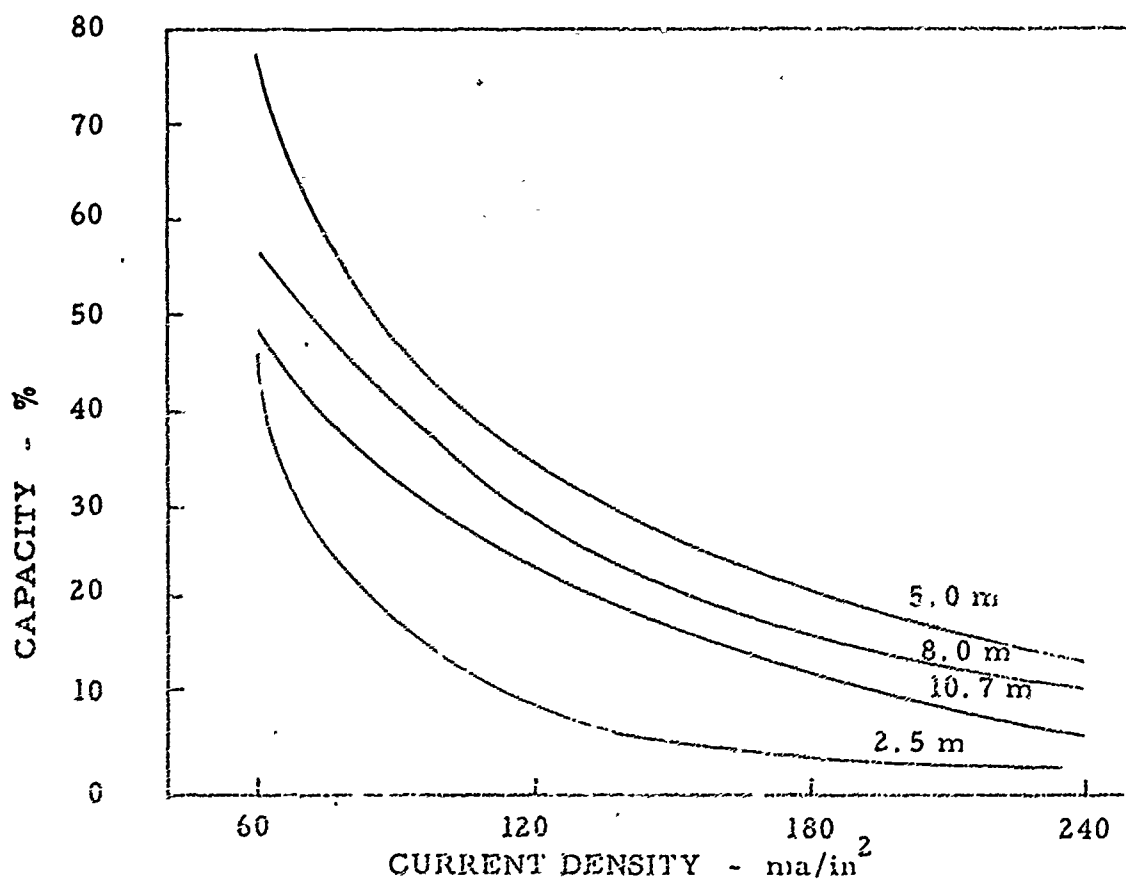


Figure 12. Effect of current density on capacity of zinc plates discharged at 0° C

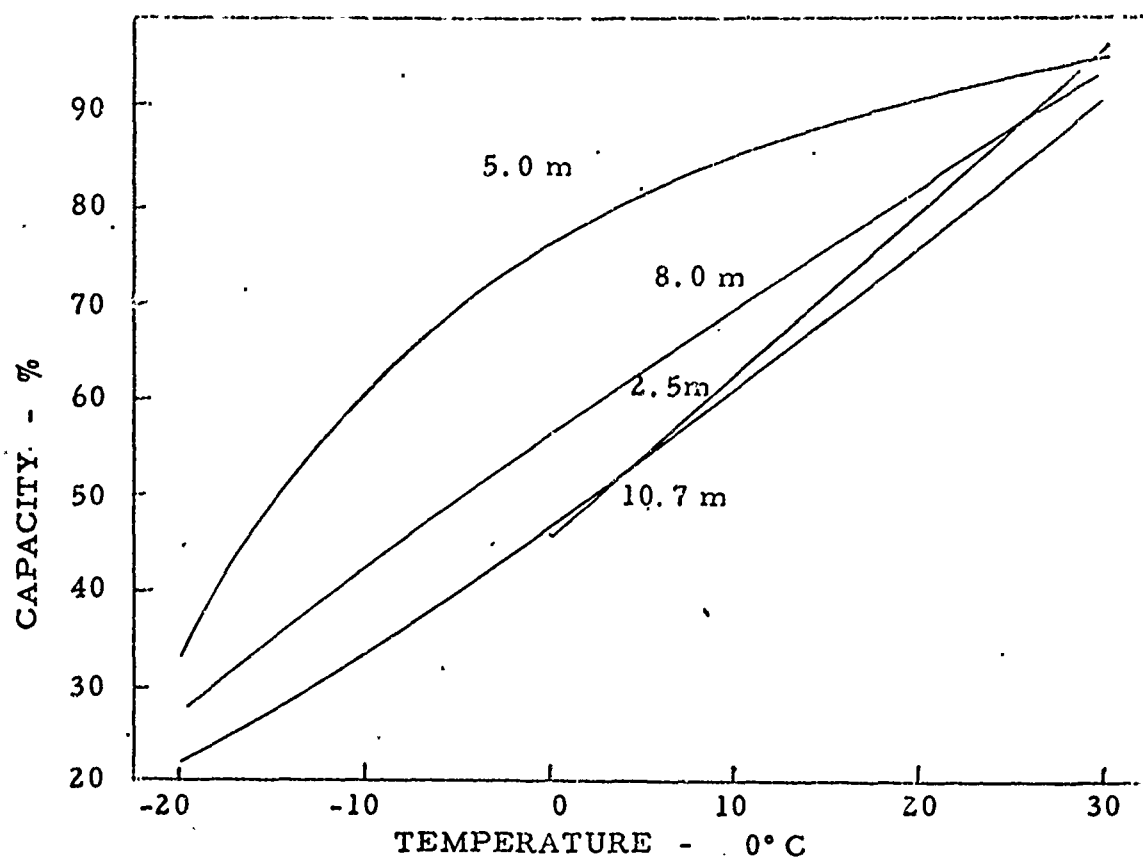


Figure 13. Effect of temperature on capacity of zinc plates discharged at 60 ma/in<sup>2</sup>.

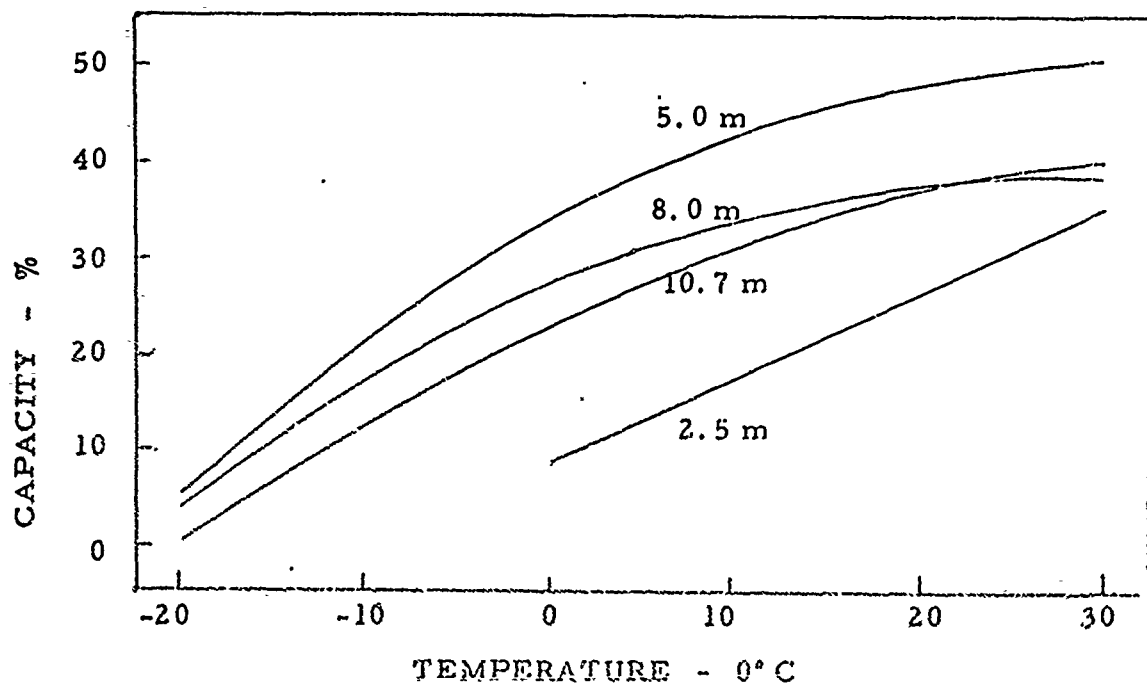


Figure 14. Effect of temperature on capacity of zinc plates discharged at 240 ma/in<sup>2</sup>.

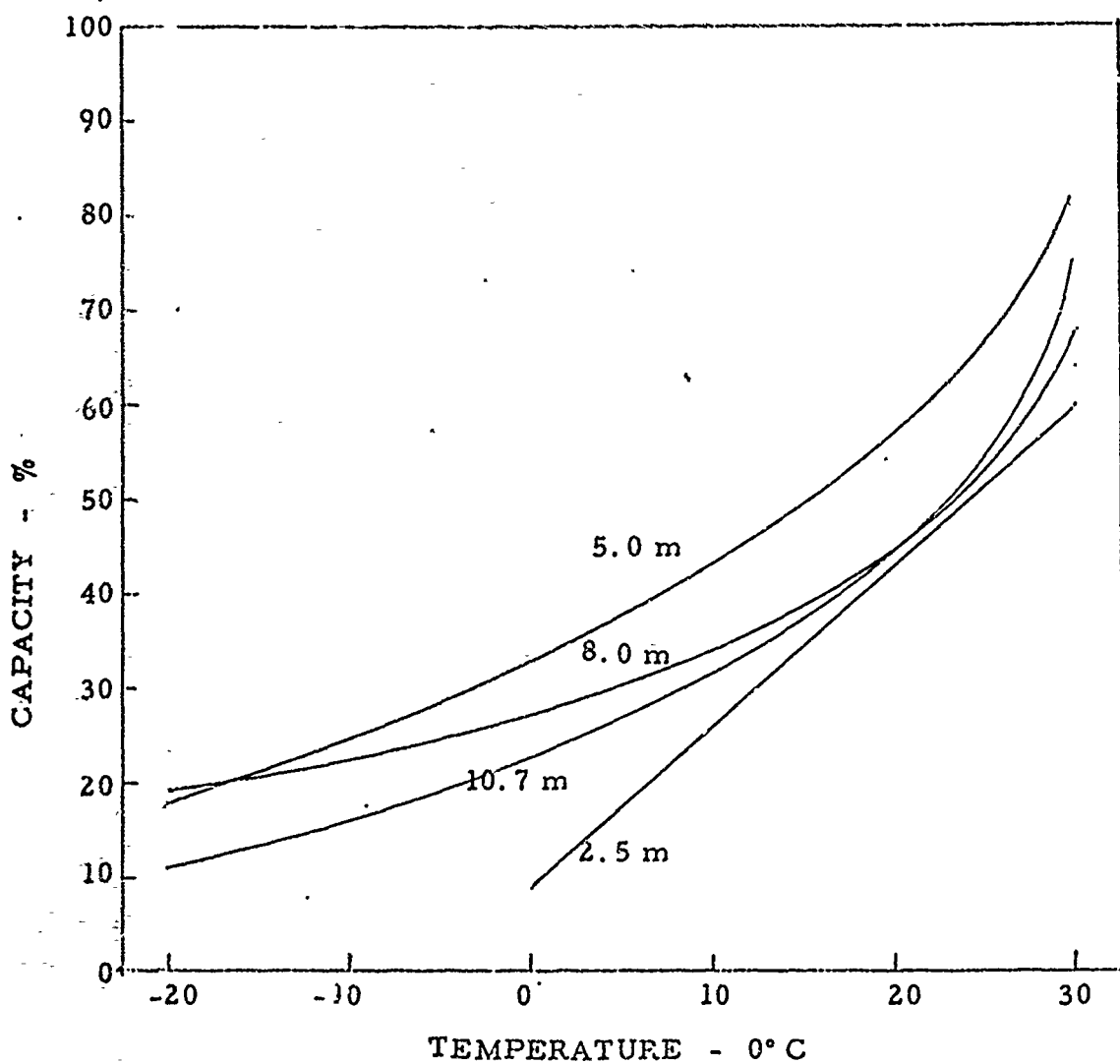


Figure 15. Effect of temperature on capacity of zinc plates discharged at 120 ma/in<sup>2</sup>.



to the increased zincate solubility at higher concentrations. The importance of this concentration effect denotes the necessity of further testing in order to determine if it was merely an artifact of the present test method, or represents a real characteristic of the zinc plate.

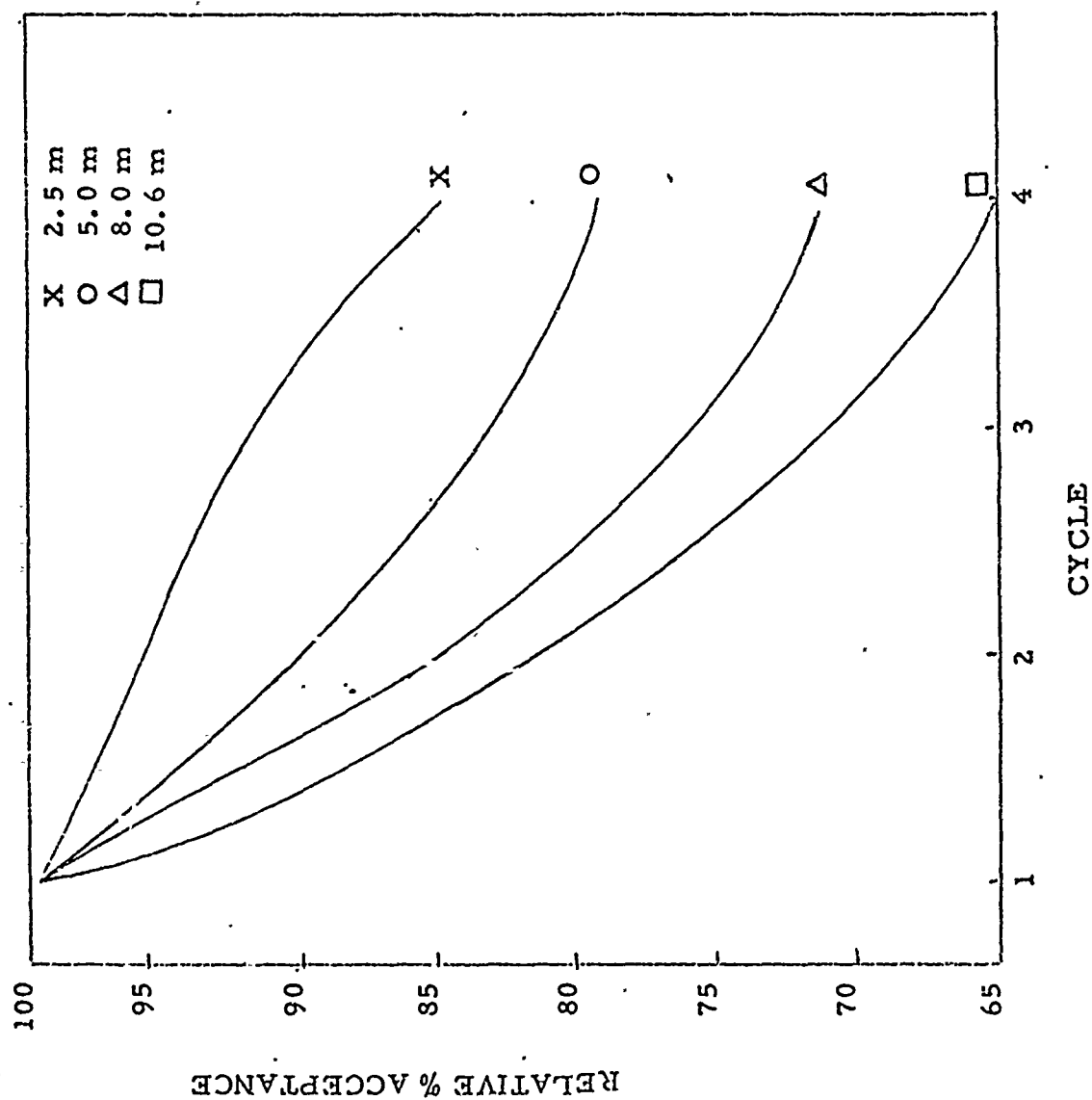


Figure 16. Effect of cycle on charge acceptance of zinc plates.

### III. DISCUSSION

The results reported herein comprise the second part of an overall effort to provide design data for construction and operation of alkaline cells. During the first year's work, the electrolyte transport and absorption characteristics of certain membranes were determined. Differential equations were derived which described the quantitative changes in anolyte and catholyte concentrations. Since these were too difficult to solve by direct methods, an iterative method was used. The transport and absorption data, together with design and operational parameters of a typical silver oxide-zinc battery, provided numerical constants for the iterative solutions. The final result was a graphical description of the anolyte and catholyte concentration vs discharge time.

The present effort comprised a study of the charge and discharge characteristics of silver, cadmium, and zinc plates. Measurements were made with respect to temperature, current density, and electrolyte concentration. The purpose of this work was not merely to obtain a qualitative measure of the effect of the variables on the plate characteristics, but to obtain a more quantitative relationship. In order to eliminate as much as possible the effects of plate to plate variation, standard methods of plate formation were used. The effects of temperature, current density, and electrolyte concentration could then be expressed on a relative basis. Choice of an average nominal plate capacity then afforded a complete time-voltage relationship.

With the results of the second year's efforts now available, it is possible to predict what the overall performance of silver oxide-zinc, silver oxide-cadmium batteries will be under certain operating conditions. This involves the combination of the concentration-time relationships derived during the initial study, together with the voltage-time curves (at various

concentrations) obtained in the present work, to yield a final voltage-time curve for the battery.

Before describing the method used to combine the results of the two years work, one point should be clarified. All design and operational parameters, such as number and size of plates, total electrolyte added, current density, and temperature, are essentially fixed at the initiation of the calculation. They may, of course, be altered for another set of calculations. The only real variables are capacity, voltage regulation, and concentration. Even these are not real variables in that the final voltage-time curve for the battery will be dependent upon the choice of the design and operational parameters. There are, therefore, two classes of variables which must be considered in the calculations. As the first step in the correlation of the two years effort, it is necessary to choose a typical battery design and set of operating parameters. Anolyte and catholyte concentration-time curves are then derived from this data and the membrane transport and absorption characteristics. This was essentially the final result of the first years efforts. The design and operating parameters used for the calculations are listed below:

Total negative plate area -  $120 \text{ in}^2$

Current density -  $133 \text{ ma/in}^2$

Type of membrane - Visking V-7

Layers of membrane - 4

Temperature -  $0^\circ \text{C}$

Amount of electrolyte - 140 g

Concentration of added electrolyte - 9.0 m

As will be seen, the only parameter which does not correspond to the concentration-voltage data is that of current density. Direct measurements

of plate capacities and voltages were made at  $120 \text{ ma/in}^2$ . However, we do not feel that the difference will have a marked effect on the results. We have also chosen to use linear extrapolation of the concentration-time curves to extend the time range into the region which corresponded to the full plate discharge. Some trial runs had previously indicated that this was an acceptable method. An illustration of the extrapolated curves is shown in Figure 17. The use of previously determined computer derived data markedly facilitated this correlation. Although expanded computer facilities have recently been installed at Whittaker R & D, new programming would be rather time consuming for an initial correlation. The expanded computer capability would facilitate a more complete study, of course.

The second step in the correlation primarily involves the results of the second year's work. This is a set of voltage-time curves at varying concentrations, but at fixed current density and temperature. The choice of the latter two parameters corresponds to the values used in the first step. This set, for zinc plates under the test conditions is shown in Figure 18.

The third step in the correlation is to establish a voltage-concentration plot at certain time values. This is accomplished from the voltage-time curve by following the voltage-concentration change at definite times. The resultant family of curves is shown in Figure 19. As is readily noted, there is a certain area of uncertainty, represented by the dashed lines. This is due to the fact that the exact cell dropoff is not known in all cases. We have used a simple extrapolation to 0.0 v to present the dashed lines, as a matter of convenience.

The last step in the correlation combines the use of Figure 17 and Figure 19. From Figure 17 the concentration at a specific time is found. Using this value of the concentration, together with the time value, a value of

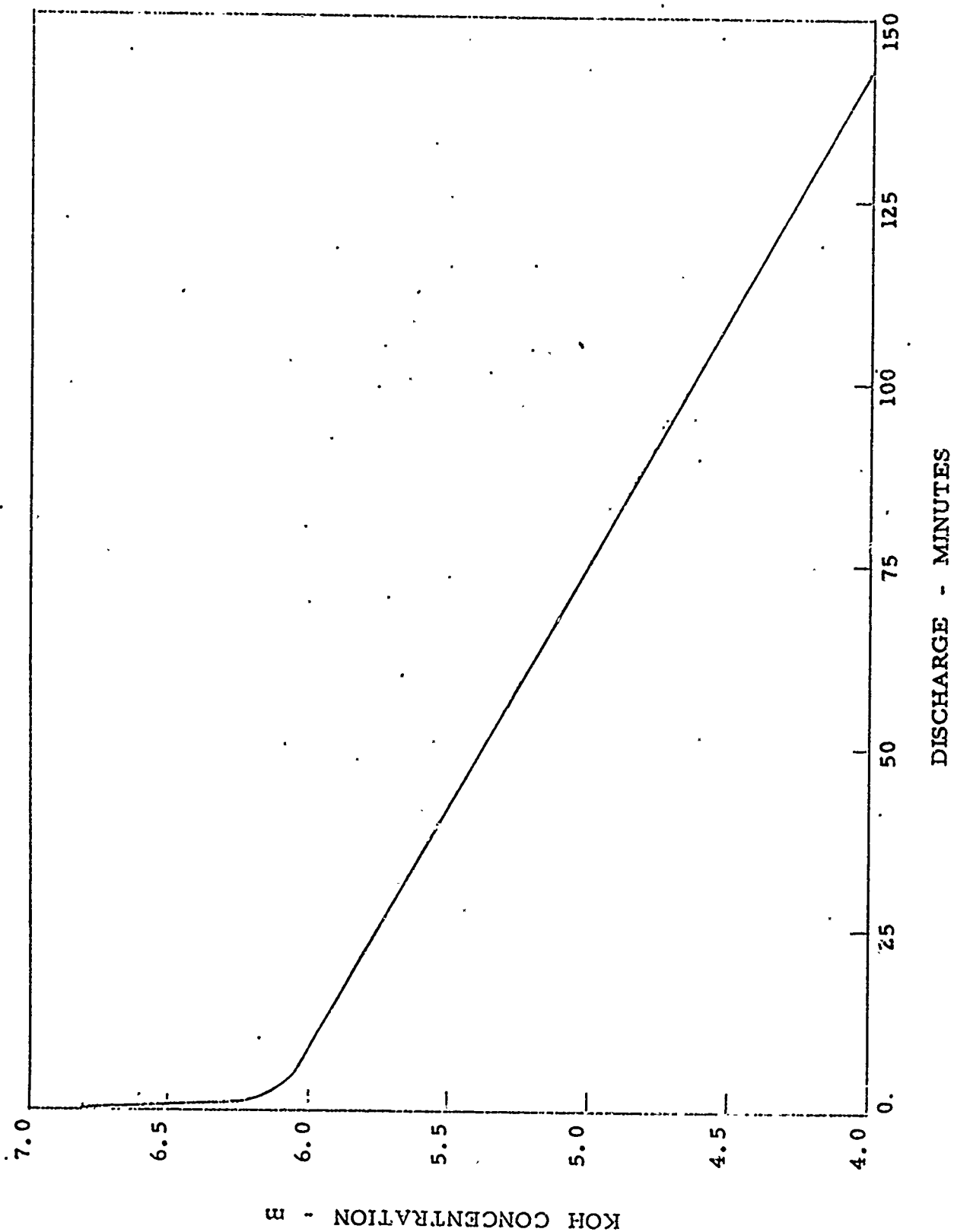


Figure 17. Change of anolyte concentration on discharge.

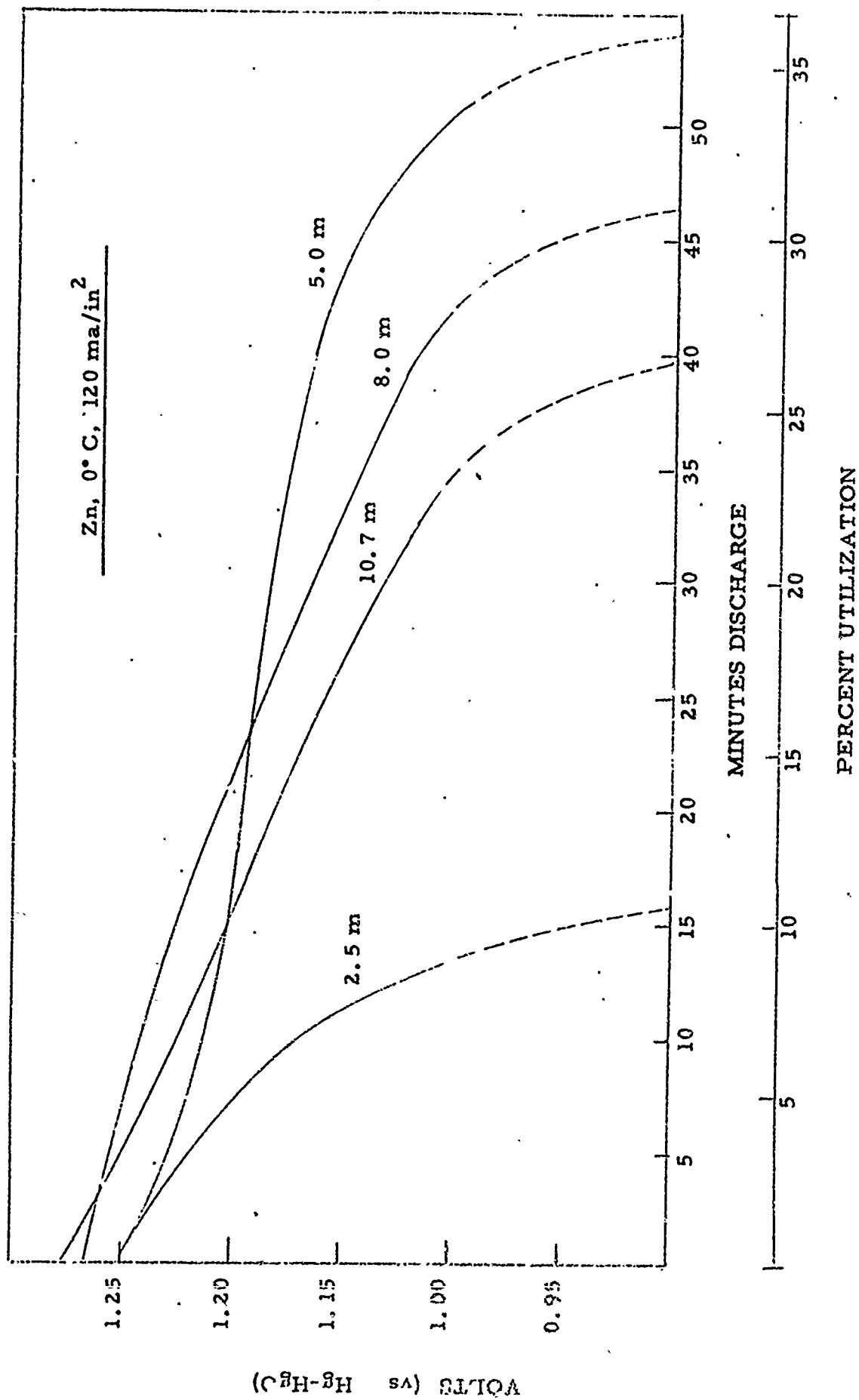


Figure 18. Effect of concentration on discharge characteristics

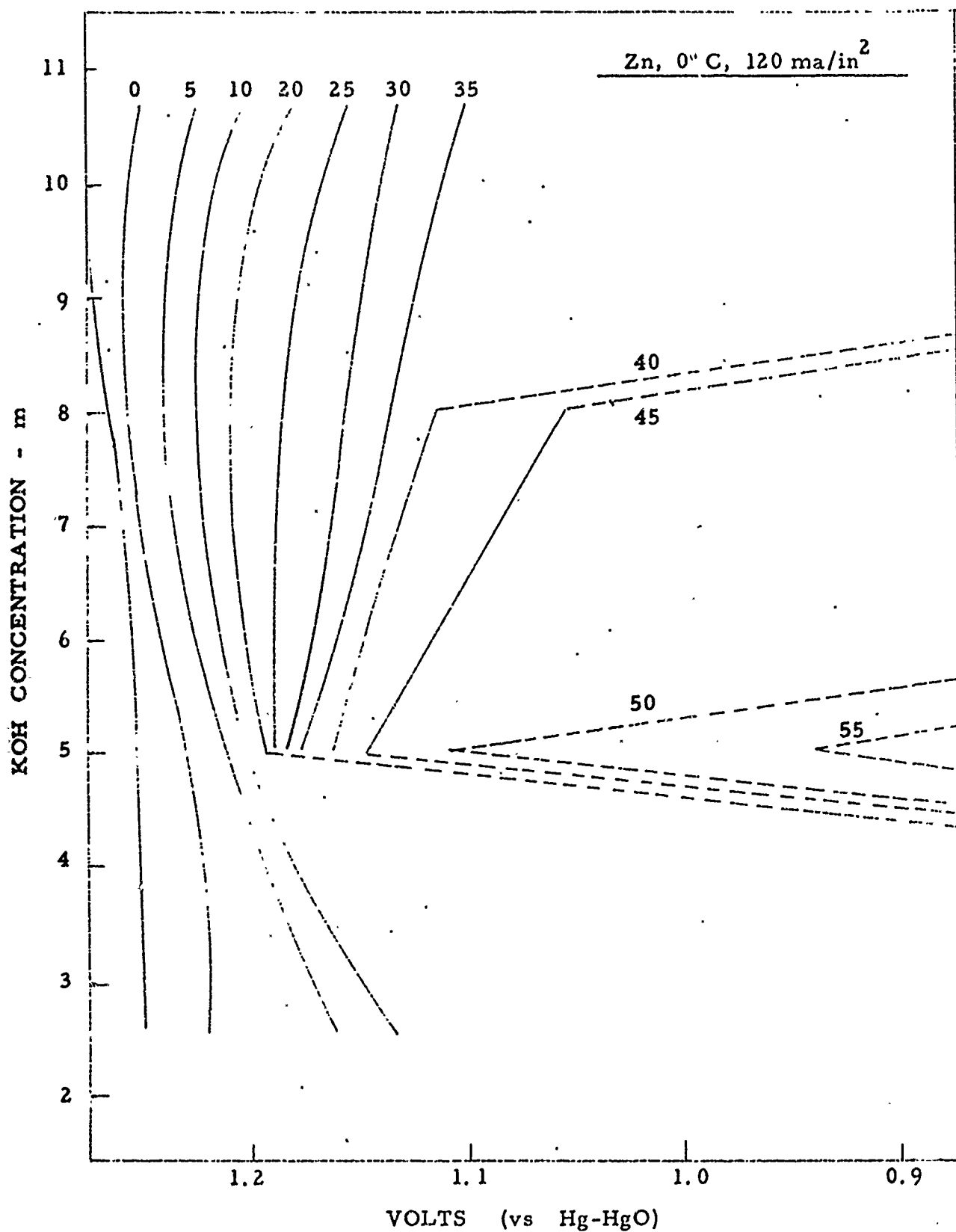


Figure 19. Effect of concentration on voltage.



the voltage is determined from Figure 19. The voltage-time point is then entered on a new figure. This process is then repeated until the entire voltage-time curve has been generated, (curve a, Figure 20). For comparison, calculations were made for the same cell at 30° C (curve b, Figure 20) and for the cell at 0° C, in which six layers of membrane are used (curve c, Figure 20). Figure 4 presents the entire expected characteristics of a silver-zinc battery. No direct calculations were made for the silver plate, since it had been found that little polarization or loss of capacity existed for the silver plate under the test conditions.

The sample correlation is for a single complete discharge. However, the method is not limited to discharge but may be readily used for the charge reaction. Furthermore, it may be used to describe the cell characteristics at less than 100% depth of discharge. At present, we are able to predict cell characteristics for silver oxide-zinc and silver oxide-cadmium batteries. The method may also be applied to alkaline fuel cells and hybrid fuel cells such as the zinc-air couple. Use in the latter two instances would, of course, necessitate compilation of additional electrode data.

There are certain assumptions which have been used in the determination of the correlation. However, it is believed that within the limits of the method and present results, a reasonably sound scientific basis has been developed for evaluating design and operational characteristics of alkaline power sources. It would appear that actual evaluation of the method would form the most important part of the work.

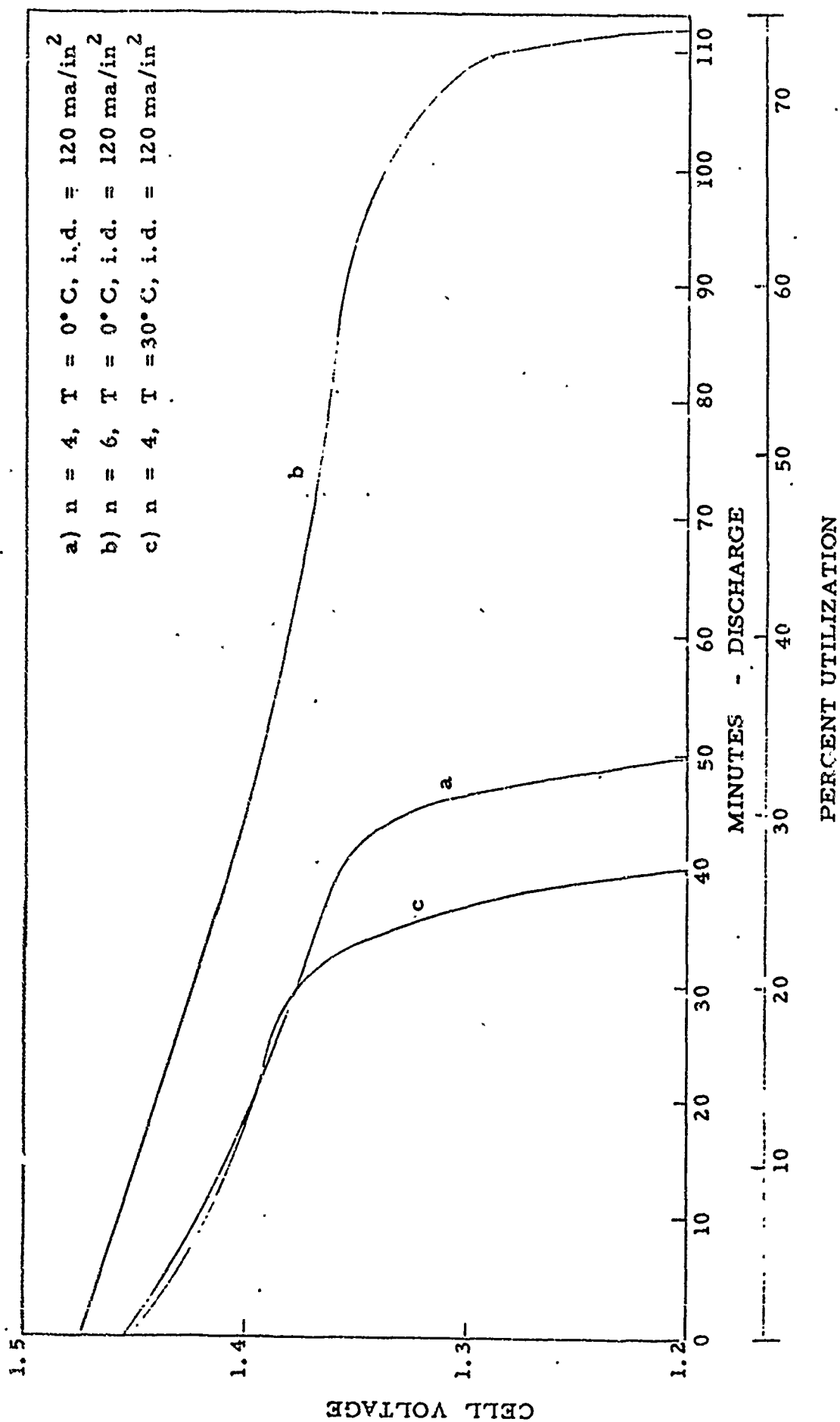


Figure 20. Predicted discharge characteristics - Silver oxide-zinc battery.

#### IV. RECOMMENDATIONS

Initially it was stated that there were essentially two areas of endeavor that should be further explored. The first area involves direct application of the derived methods to actual batteries. The second area essentially comprises a refinement and extension of the data obtained in the first two years work.

One necessary item is the determination of the effect of storage on the transport and absorption characteristics of membranes. This involves storage in complete batteries as opposed to simple electrolyte. As an adjunct to this effort, is the correlation of the effect of a charge-discharge regimen on the membrane parameters. It is not expected that it would be necessary to run as complete a series of determinations as was accomplished during the first year. A series of spot-checks would probably reveal any marked effects of storage and/or cell operation on the membrane parameters.

A second area that needs investigation is the effect of zincate ion on both the membrane transport characteristics and on the reaction stoichiometry used in the derivation of the gradient equations. The effect of zincate ion could markedly alter the transport characteristics of the membrane. Furthermore, presence of zincate ion necessarily alters the reaction stoichiometry. This must be taken into account during the determination of electrolyte concentration-time relationships as shown in Figure 7. The problem of zincate concentration effects is further complicated by the fact that zincate ion is not merely formed at the zinc electrode, but is absorbed by the membrane and diffuses into the silver electrode chamber. Fortunately, there have been measurements of zincate absorption and diffusion

characteristics of typical battery separators. Correlation of the zincate parameters with the cell data is expected to improve the accuracy of the design calculations.

Although it is not evident from Figure 7, some preliminary calculations indicate that overall loss of electrolyte from the anolyte may be sufficient to cause "drying out" of the zinc plates. This phenomena has been suspected as a cause of capacity loss but has not been previously quantitized. It is now possible to determine, with some measure of accuracy, what total quantities of free electrolyte are necessary for battery or fuel cell operation.

Although several interesting electrode characteristics were revealed during the second year's effort, two features are of primary import for the proposed design study. The first of these is the lack of second plateau charge acceptance of the silver electrode under certain conditions. Although some measure of the quantitative limitations of this effect are known, additional effort to demarcate this phenomena would be of value.

A second area is concentration dependent loss of charge acceptance of zinc plates on cycling. Although the number of cycles which was used to condition the plates before the test runs was limited, it was evident that there was a decrease in charge acceptance on each successive cycle. This effect appeared to be dependent on the electrolyte concentration. This may have been an artifact which was due to the necessary use of excess electrolyte in the tests. However, it is of sufficient importance so as to warrant further study under electrolyte limited conditions.

These are some of the ancillary areas which are expected to aid in the development of suitable methods for the sound engineering design of silver oxide-zinc and other alkaline power sources. Specific choice and priority

of investigation is open at this time. This present effort has merely endeavored to present some of the salient features related to the development of adequate design data for alkaline batteries and fuel cells.

## V. REFERENCES

1. Whittaker Corp., Narmco R & D Div., Final Report  
Contract No. D-R 108650, August 1966 - July 1967 in Fifth Quarterly  
Report, Delco-Remy Div., General Motors Corp., October 1967,  
Contract No. AF 33(615)-3487.
2. E. J. Casey and W. J. Moroz, Can. J. Chem., 43, 1199 (1965)

UNCLASSIFIED

Security Classification

DOCUMENT CONTROL DATA - R&D		
(Security classification of title, body of abstract and indexing annotation must be entered when the overall report is classified)		
1. ORIGINATING ACTIVITY (Corporate author) Delco-Remy Division General Motors Corporation Anderson, Indiana		2a. REPORT SECURITY CLASSIFICATION Unclassified
		2b. GROUP
3. REPORT TITLE  Silver-Zinc Electrodes and Separator Research		
4. DESCRIPTIVE NOTES (Type of report and inclusive dates)  * 1 July 1968 to 1 October 1968		
5. AUTHOR(S) (Last name, first name, initial)  J. A. Kerala		
6. REPORT DATE October 15, 1968	7a. TOTAL NO. OF PAGES	7b. NO. OF REFS
8a. CONTRACT OR GRANT NO. AF33(615)-3487	8a. ORIGINATOR'S REPORT NUMBER(S)	
b. PROJECT NO.		
c.	8b. OTHER REPORT NO(S) (Any other numbers that may be assigned this report)	
d.		
10. AVAILABILITY/LIMITATION NOTICES Foreign announcement and dissemination of this report by DDC is not authorized.		
11. SUPPLEMENTARY NOTES		12. SPONSORING MILITARY ACTIVITY Aero Propulsion Laboratory, Research and Technology Div., Air Force Systems Command Wright-Patterson AFB, Ohio
13. ABSTRACT <p>Twenty-five a.h. cells are under cycle test containing 90 Mrad crosslinked methacrylic acid radiated graft. These cells contain three, four and five layers of this membrane. Cells constructed with rectangular voids at the plate centers have been cycled at 60% DOD with some success, but in general the results have not been exceptional.</p> <p>Cells containing .3% Al doped ZnO and .25% Pb doped ZnO as negative active material delivered 212 and 190 cycles respectively at 60% DOD.</p>		

DD FORM 1473  
1 JAN 64

Security Classification